

## Self-polarization fields of rare-earth impurities in $s$ - $p$ hosts: A theoretical study

A. Troper, O. L. T. de Menezes, P. Lederer,\* and A. A. Gomes

Centro Brasileiro de Pesquisas Físicas, Avenida Wenceslau Braz, 71, 20.000 Rio de Janeiro, RJ, Brazil

(Received 28 February 1978)

A model consisting of an Anderson-Moriya  $d$  resonance, strongly perturbed by a Slater-Koster potential acting in the conduction band, is developed to describe dilute rare-earth impurities in  $s$ - $p$  hosts. The properties of this model are studied, in particular the deviations from the usual behavior of the phase shifts due to the Slater-Koster potential. The local magnetic responses to the rare-earth's exchange fields are calculated in order to discuss self-polarization hyperfine fields of the rare earth in these hosts. The behavior of the hyperfine fields in terms of the parameters of the model is discussed numerically and possible changes in sign along the  $s$ - $p$  series are obtained. It is suggested that the combination of an Anderson-Moriya resonance and the strong Slater-Koster scattering may be a physical mechanism suitable to induce changes in sign of the hyperfine field in these systems. Experiments are suggested to test the model.

### I. INTRODUCTION

Magnetic-rare-earth impurities have been used successfully as probes in host metals in several experimental works. In particular, hyperfine-field measurements have been reported in the literature for transition-metal hosts<sup>1-3</sup> or inter-metallics.<sup>2,4</sup>

From the theoretical point of view diluted magnetic-rare-earth impurities in such transitionlike host metals have been interpreted as physical realizations of simultaneous presence at the same site of charge-impurity scattering and exchange polarization.<sup>5,6</sup>

In this work we want to discuss theoretically the problem of a magnetic-rare-earth impurity embedded in  $s$ - $p$  hosts. Contrary to the problem discussed in Ref. 6 where there exists a considerable amount of experimental data,<sup>2,7</sup> to our knowledge experimental data concerning hyperfine-field measurements at the nuclei of rare-earth impurities in  $s$ - $p$  hosts have not been reported in the literature.

The case of a magnetic-rare-earth impurity diluted in  $s$ - $p$  hosts contrasts with the previous transition-metal case<sup>5,6</sup> due to the absence of unfilled  $d$  bands in the neighborhood of the Fermi level of the host. However, the existence of filled  $d$  bands near the bottom of the pure host  $s$ - $p$  band provides the possibility of extracting  $d$  bound states from it, as in the case of transition impurities in Cu or Al.<sup>8</sup>

Hence, the existence of  $d$  states, i.e., a  $d$ -virtual-bound-state hump near the Fermi level apart from the host conduction  $s$ - $p$  states is an impurity effect.

One has experimental evidence confirming the existence of a  $d$  virtual bound state for rare earths diluted in some noble metals (Ag and Au). Measurements of skew scattering of rare-earth im-

purities in these noble metals<sup>9</sup> show that the maximum value is obtained for Gd impurities. Since Gd is an S-like ion, the usual anisotropic exchange scattering as derived by Kondo<sup>10</sup> (and reported in Ref. 9) vanishes since the angular momentum is zero. The apparent contradiction is resolved by introducing a  $5d$  virtual bound state and including spin-orbit coupling of these electrons. Other evidence is provided by studies of the sign of the crystalline-field coefficients.<sup>11</sup>

The rare-earth valence plays a central role in the problem we discuss throughout this work. In fact, for trivalent rare atoms the number of  $d$  electrons per impurity in the  $d$  hump plus the number of conduction states is equal to 3, whereas for divalent impurities the sum is 2. If one studies a series of  $s$ - $p$  metals one then varies the number of  $s$ - $p$  electrons in the host from, say, 2 to 7. Then a repulsive potential must ensure the correct change of number of  $s$ - $p$  electrons per rare-earth impurity and thereby the resonating  $d$  bound state is strongly modified by this extra charge potential. In other words, a  $d$  atomic Anderson state<sup>12</sup> mixes to a Slater-Koster (SK)<sup>13</sup> perturbed conduction density of states, thus affecting the "effective width" and height of the  $d$  hump. So we suggest that a Friedel-Anderson (FA) model where the conduction states are perturbed is physically realized when trivalent-rare-earth impurities are diluted in  $s$ - $p$  hosts.

If one concentrates on hyperfine results in these systems we argue that the trivalent-rare-earth  $4f$  magnetic moment polarizes both the Moriya-like distorted  $d$  hump<sup>14</sup> and the SK perturbed host density of states.

In this work we are concerned with S-state rare earths, otherwise the strong orbital hyperfine field should be present. So our results apply to Gd<sup>3+</sup> (or Eu<sup>2+</sup>) impurities.

The theoretical problem discussed in this work

contrasts with the transition-metal-host case<sup>5,6</sup> where the rare-earth  $4f$  moment polarizes the perturbed  $d$ -band host (mostly responsible for the excess charge screening) and the  $s$  band, which feels impurity effects only via  $s$ - $d$  scattering. In that case it was shown<sup>6</sup> that no change in sign of the hyperfine field as a function of the charge difference was possible. Moreover, the sign of the hyperfine field was determined only by the sign of the exchange coupling between  $d$  conduction states and  $f$  localized states in agreement with ESR experiments.<sup>2,7,15</sup>

In the  $s$ - $p$  host case,  $d$ -electron occupation is small. One hopes that in favorable situations change in sign may occur since competitive mechanisms (contact and core polarizations) may become comparable and alternate in importance.

Our paper has five sections. Sections II and III are dedicated to the formal aspects. In Sec. II we present the model, whereas Sec. III contains the general mathematical treatment of the problem and basic derivations of the hyperfine contributions. In Sec. IV we describe and discuss the numerical results obtained. Concluding remarks are made in Sec. V.

## II. THEORETICAL MODEL

In this section we describe the main ingredients of the model, e.g., the unperturbed  $s$ - $p$  host and the impurity potential introduced by the magnetic-rare-earth impurity. Let us start with the unperturbed  $s$ - $p$  host. One adopts a simplified band model based in Campbell's<sup>16</sup> picture for  $s$ - $p$  impurities embedded in ferromagnetic hosts. This model consists of eight identical subbands, each one normalized to unity in order to account for the filling of the  $s$ - $p$  series. Within this particular model, the peculiar  $s$  or  $p$  character as obtained from decomposition of the total density of states<sup>16</sup> is replaced by a uniform distribution with weights of, respectively,  $\frac{2}{8}$  and  $\frac{6}{8}$  for the  $s$  and  $p$  densities of states. Then, in the Wannier representation the one-electron Hamiltonian for one conduction subband is

$$\mathcal{H}_{\text{host}} = \sum_{ij\sigma} T_{ij} c_{i\sigma}^\dagger c_{j\sigma}, \quad (2.1)$$

where  $c_{i\sigma}^\dagger$  and  $c_{i\sigma}$  are, respectively, the creation and annihilation operators for electrons with spin  $\sigma$  at the  $i$ th Wannier site in that subband;  $T_{ij}$  is the transfer integral between sites  $i$  and  $j$  defined by

$$T_{ij} = \sum_{\mathbf{k}} \epsilon_{\mathbf{k}} e^{i\mathbf{k} \cdot (\mathbf{R}_i - \mathbf{R}_j)}, \quad (2.2)$$

$\epsilon_{\mathbf{k}}$  being the band energy.

Now we describe the impurity effects. These are separated into two types: potential scattering of the  $s$ - $p$  states and resonance effects associated to a  $d$  atomic state.

As far as the first effect is concerned one assumes that the trivalent-rare-earth impurity is characterized by  $Z_{\text{imp}}^{(c)}$  and  $Z_{\text{imp}}^{(d)}$ , i.e.,  $s$  and  $d$  configurations, respectively, with  $Z_{\text{imp}}^{(c)} + Z_{\text{imp}}^{(d)} = 3$ . The values of  $Z_{\text{imp}}^{(c)}$  and  $Z_{\text{imp}}^{(d)}$  will be discussed in more detail later on. Starting from atomic values one has, e.g., Gd atoms  $Z_{\text{imp}}^{(c)} = 2$  and  $Z_{\text{imp}}^{(d)} = 1$ . Then, if the rare-earth impurity is embedded in a metal with  $Z_h$   $s$ - $p$  electrons, a repulsive impurity potential should be introduced in order to repel  $Z_h - Z_{\text{imp}}^{(c)}$  electrons. These remarks define (i) a SK problem specified by the potential  $V_{cc}$  assumed to be localized at the impurity site, so that

$$\mathcal{H}_{\text{imp}}^{(c)} = \sum_{\sigma} V_{cc} c_{0\sigma}^\dagger c_{0\sigma}. \quad (2.3)$$

The strength of the impurity-induced scattering matrix element  $V_{cc}$  is determined self-consistently as a function of the charge difference  $\Delta Z_c = Z_h - Z_{\text{imp}}^{(c)}$  through Friedel's sum rule,<sup>17</sup>

$$\Delta Z_c = \frac{8}{\pi} \arctan \frac{\pi V_{cc} \rho_c(\epsilon_F)}{1 - V_{cc} F_c^R(\epsilon_F)}. \quad (2.4)$$

In (2.4) the factor 8 accounts for  $s$ - $p$  degeneracy, whereas  $\rho_c(\epsilon_F)$  and  $F_c^R(\epsilon_F)$  are, respectively, the density of states and Hilbert transform at the Fermi level of the conduction subband suitably normalized to 1. Clearly, if the  $s$  and  $p$  densities of states are available from a band calculation, (2.4) should be replaced by the corresponding equations describing  $s$  and  $p$  contributions to screening.

(ii) The second contribution to the charge-impurity problem arises from the existence in  $s$ - $p$  metals of a filled  $d$  band (10 electrons) lying far below the  $s$ - $p$  Fermi level.

We assume that the existence of the atomic  $5d$  level of the rare earth provides a locally strong repulsive potential capable of extracting a bound state from this filled  $d$  band. The repelled bound state resonates then with the conduction states, producing a virtual bound state around the Fermi level. The Hamiltonian associated to the resonating "atomic"  $d$  level is

$$\mathcal{H}_{\text{imp}}^{(d)} = \sum_{\sigma} \epsilon_d d_{0\sigma}^\dagger d_{0\sigma} + \sum_{\sigma} (V_{cd} c_{0\sigma}^\dagger d_{0\sigma} + V_{dc} d_{0\sigma}^\dagger c_{0\sigma}) + U_{dd} n_{0d}^{(d)} n_{0d}^{(d)}; \quad n_{0\sigma}^{(d)} = d_{0\sigma}^\dagger d_{0\sigma}, \quad (2.5)$$

where  $d_{0\sigma}^\dagger$ ,  $d_{0\sigma}$  are creation and annihilation operators for the  $d$  local states (in Anderson's sense<sup>10</sup>) located at the origin and with energy  $\epsilon_d$ .  $V_{cd}$  and  $V_{dc}$  are the matrix elements accounting for the broadening of the local level and  $|V_{cd}|^2$  is one of the parameters of our model. Finally  $U_{dd}$

is the local Coulomb repulsion. The impurity effects associated to the rare-earth impurity are then incorporated in the Hamiltonian

$$\mathcal{H}_{\text{imp}}^{\text{ch}} = \mathcal{H}_{\text{imp}}^{(c)} + \mathcal{H}_{\text{imp}}^{(d)}. \quad (2.6)$$

It is assumed throughout that a nonmagnetic Hartree-Fock solution is obtained for the extended Anderson-Moriya (AM) problem defined by (2.1), (2.3), and (2.5). As far as self-polarization hyperfine fields are concerned, the existence of the local Coulomb interaction  $U_{dd}$  between  $5d$  electrons amounts to weak Hartree-Fock enhancement of the local magnetic response of  $d$ -hump states to the exchange interaction with the  $4f$  moment (see Sec. IV). In this work we neglect this effect, which tends to increase the  $d$  contribution to the hyperfine field.

For a given hybridization matrix element  $|V_{cd}|^2$  and band-structure model [given by the density of states  $\rho_c(\omega)$  and the corresponding Hilbert transform  $F_c^R(\omega)$ ], the problem for a spinless rare-earth impurity like Lu is completely specified by determining self-consistently the position  $\epsilon_d$  of the  $d$  atomic state with respect to the Fermi level. To do that one should solve the AM problem in presence of the SK perturbed  $s$ - $p$  states. This will be done in Sec. III and here we just state the result for the self-consistency equation. The number of states associated to the resonant states ( $d$  hump plus conduction-state contribution) is given by

$$\Delta Z_d = \frac{10}{\pi} \arctan \frac{\pi |V_{cd}|^2 \tilde{\rho}_{c,0}(\epsilon_F)}{\epsilon_F - \epsilon_d - |V_{cd}|^2 \tilde{F}_{c,0}^R(\epsilon_F)}. \quad (2.7)$$

The factor 10 accounts for the  $d$ -level degeneracy, whereas  $\tilde{\rho}_{c,0}(\epsilon_F)$  and  $\tilde{F}_{c,0}^R(\epsilon_F)$  are, respectively, the local SK perturbed density of states and its Hilbert transform at the Fermi level. The self-consistent determination of  $\epsilon_d$  goes as follows: using the value of the Fermi energy  $\epsilon_F$  associated to the host  $s$ - $p$  metal with  $Z_h$  electrons and imposing  $\Delta Z_d = 1$ , one gets from (2.7) the value of  $\epsilon_d$ .

If the impurity is a magnetic rare earth like Gd, the localized  $f$  moment polarizes both the perturbed  $s$ - $p$  conduction states and the  $d$  hump. The coupling term is as usually

$$\mathcal{H}_{\text{imp}}^{\text{exch}} = -\frac{1}{2} \sum_{\sigma} \sigma \langle S^z \rangle (J^{(c)} c_{0\sigma}^{\dagger} c_{0\sigma} + J^{(d)} d_{0\sigma}^{\dagger} d_{0\sigma}), \quad (2.8)$$

where  $J^{(\lambda)}$  (for  $\lambda = c$  or  $d$ ) are, respectively, the exchange interactions between the localized  $4f$  state and the  $s$ - $p$  conduction states or  $d$  states. For simplicity's sake, the  $\mathbf{k}, \mathbf{k}'$  dependence of these couplings is completely disregarded and as discussed below (cf. Sec. IV) these parameters

enter in our calculation through the ratio  $J^{(d)}/J^{(c)}$ .

Hence, our model Hamiltonian describing a magnetic rare earth embedded in a metallic  $s$ - $p$  host is given by

$$\mathcal{H} = \mathcal{H}_{\text{host}} + \mathcal{H}_{\text{imp}}^{\text{ch}} + \mathcal{H}_{\text{imp}}^{\text{exch}}. \quad (2.9)$$

### III. FORMALISM

#### A. General mathematical approach

In order to obtain the contact and core contributions to the self-polarization hyperfine field at the rare-earth impurity nucleus we calculate the  $s$ - $p$  conduction electron and  $d$ -hump magnetizations induced by the local  $f$  moment  $\langle S^z \rangle$  at the rare-earth impurity site. This calculation will be performed in the Born approximation for the "local exchange fields"  $V_{\text{exch}}^{(\lambda)} = -\frac{1}{2} \sigma J^{(\lambda)} \langle S^z \rangle$  ( $\lambda = c$  or  $d$ ). To do that we must determine the complete Green's function matrix elements  $\Gamma_{00\sigma}^{cc}(\omega)$  and  $\Gamma_{00\sigma}^{dd}(\omega)$  associated with the Hamiltonian (2.9).

We start from the unperturbed system (i.e.,  $\mathcal{H} = \mathcal{H}_{\text{host}}$ ): to a given conduction subband of the pure host described by (2.1) corresponds a Green's function  $\hat{g}(\omega)$ , the elements of which are given by

$$g_{ij}^{cc}(\omega) = \sum_k \frac{e^{ik(R_i - R_j)}}{\omega - \epsilon_k}. \quad (3.1)$$

Due to the translational invariance of the pure host, the diagonal elements  $g_{ii}^{cc}(\omega)$  are independent of site  $i$  and are connected to the Hilbert transform of the unperturbed  $s$ - $p$  density of states through

$$g_{ii}^{cc}(\omega) = g_{00}^{cc}(\omega) = F_c(\omega) = \sum_k \frac{1}{\omega - \epsilon_k} = \int_{E_b}^{E_t} \frac{\rho_c(\omega')}{\omega - \omega'} d\omega', \quad (3.2)$$

$E_b$  and  $E_t$  being, respectively, the bottom and the top of the  $s$ - $p$  subband.

In (3.2) one has real and imaginary parts. Hence

$$F_c(\omega + i\zeta) = F_c^R(\omega) - i\pi\rho_c(\omega) \quad (\zeta \rightarrow 0^+), \quad (3.3a)$$

where

$$F_c^R(\omega) = \mathcal{P} \sum_k \frac{1}{\omega - \epsilon_k} = \mathcal{P} \int_{E_b}^{E_t} \frac{\rho_c(\omega')}{\omega - \omega'} d\omega', \quad (3.3b)$$

$\mathcal{P}$  being Cauchy's principal part.

When one introduces the rare-earth impurity at the origin, one gets a "perturbed" system characterized by a Green's function  $\hat{\Gamma}_{\sigma}(\omega)$ , of matrix elements  $\Gamma_{ij\sigma}^{\lambda\mu}(\omega)$  ( $\lambda, \mu = c$  or  $d$ ), which can be evaluated through a Dyson-like equation

$$\hat{\Gamma}_{\sigma} = \hat{g} + \hat{g} \hat{V}_{\sigma} \hat{\Gamma}_{\sigma}. \quad (3.4)$$

The problem defined by (3.4) is to be solved as

follows. We define an intermediate Green's function characterizing the perturbed  $s$ - $p$  band [through (2.3)] which is solution of the SK problem

$$\hat{g} = \hat{g} + \hat{g} \hat{V}^{(SK)} \hat{g}. \quad (3.5)$$

Next, one has an AM-like problem [through (2.5)], namely, a sharp  $d$  level extracted from the filled  $d$ -band host collapsing into a charge perturbed  $s$ - $p$  band. The  $d$  level is described by the Green's function  $\hat{g}(\omega)$  with matrix elements (in the absence of Coulomb interactions)

$$g_{ij}^{dd}(\omega) = \frac{\delta_{ij} \delta_{i0}}{\omega - \epsilon_d}. \quad (3.6)$$

This problem can be solved by calculating  $\hat{G}$  from  $\hat{g}$ , through

$$\hat{G} = \hat{g} + \hat{g} \hat{V}^{(AM)} \hat{G}. \quad (3.7)$$

So by solving (3.7) one accounts for the pure charge potential effects introduced by the rare-earth impurity. A similar formulation was introduced by Iglesias-Sicardi *et al.*<sup>18</sup> for studying the formation of the magnetic moment of an actinide impurity in a disordered host.

Having obtained the Green's function  $\hat{G}$ , by considering the rare earth's  $4f$  moment [through (2.7)] one finally gets

$$\hat{\Gamma}_\sigma = \hat{G} + \hat{G} \hat{V}_{\text{exch}} \hat{\Gamma}_\sigma \simeq \hat{G} + \hat{G} \hat{V}_{\text{exch}} \hat{G}, \quad (3.8)$$

where the last approximate result follows using the Born approximation for exchange scattering. Let us now detail the various stages of the calculation sketched above.

#### B. Charge-impurity effects: Exact solution of Eqs. (3.5) and (3.7)

The Green's-function matrix element  $G_{ii}^{dd}(\omega)$  is evaluated from (3.7) through

$$G_{00}^{dd}(\omega) = g_{00}^{dd}(\omega) + g_{00}^{dd}(\omega) V_{dc} G_{00}^{cd}(\omega), \quad (3.9a)$$

$$G_{00}^{cd}(\omega) = \tilde{g}_{00}^{cc}(\omega) V_{cd} G_{00}^{dd}(\omega). \quad (3.9b)$$

Eliminating  $G_{00}^{cd}(\omega)$  one obtains

$$\begin{aligned} G_{00}^{dd}(\omega) &= \frac{g_{00}^{dd}(\omega)}{1 - |V_{cd}|^2 \tilde{g}_{00}^{cc}(\omega) g_{00}^{dd}(\omega)} \\ &= \frac{1}{\omega - \epsilon_d - |V_{cd}|^2 \tilde{g}_{00}^{cc}(\omega)}, \end{aligned} \quad (3.10)$$

with

$$\tilde{g}_{00}^{cc}(\omega) = \frac{g_{00}^{cc}(\omega)}{1 - V_{cc} g_{00}^{cc}(\omega)} = \tilde{F}_{c,o}^R(\omega). \quad (3.11)$$

Expression (3.11) is derived from (3.5), i.e.,  $\tilde{g}_{00}^{cc}(\omega)$  describes the Green's function matrix element at the rare-earth impurity site, which is the exact solution of the SK problem. Note that ex-

pression (3.10) is just the classical Moriya result<sup>14</sup> of a  $d$  level hybridized with a conduction band, except that in the present case the conduction states are perturbed by the impurity potential  $V_{cc}$ .

Let us now evaluate the Green's-function matrix element  $G_{ii}^{cc}(\omega)$ .

Again from (3.7) one has

$$G_{ii}^{cc}(\omega) = \tilde{g}_{ii}^{cc}(\omega) + \tilde{g}_{i0}^{cc}(\omega) V_{cd} G_{0i}^{dc}(\omega), \quad (3.12a)$$

$$G_{0i}^{dc}(\omega) = g_{00}^{dd}(\omega) V_{dc} G_{0i}^{cc}(\omega). \quad (3.12b)$$

Eliminating  $G_{0i}^{dc}(\omega)$  yields

$$G_{ii}^{cc}(\omega) = \tilde{g}_{ii}^{cc}(\omega) + \tilde{g}_{i0}^{cc}(\omega) \frac{|V_{cd}|^2}{\omega - \epsilon_d - |V_{cd}|^2 \tilde{g}_{00}^{cc}(\omega)} \tilde{g}_{0i}^{cc}(\omega), \quad (3.13)$$

where

$$\tilde{g}_{ii}^{cc}(\omega) = g_{ii}^{cc}(\omega) + g_{i0}^{cc}(\omega) \frac{V_{cc}}{1 - V_{cc} g_{00}^{cc}(\omega)} g_{0i}^{cc}(\omega) \quad (3.14)$$

is precisely the  $i$ - $i$  Green's-function matrix element as derived from (3.5).

So, the Green's-function matrix element  $G_{00}^{cc}(\omega)$  at the impurity site is

$$G_{00}^{cc}(\omega) = \frac{(\omega - \epsilon_d) \tilde{g}_{00}^{cc}(\omega)}{\omega - \epsilon_d - |V_{cd}|^2 \tilde{g}_{00}^{cc}(\omega)}. \quad (3.15)$$

The Green's-function matrix element defined by (3.10), (3.13), and (3.14), which are obtained in terms of pure host  $s$ - $p$  band quantities [as  $\rho_c(\omega)$  and  $F_c^R(\omega)$ ] and impurity quantities (as  $V_{cc}$ ,  $\epsilon_d$ , and  $|V_{cd}|^2$ ) completely solve the  $d$ -impurity scattering problem (AM problem) in terms of  $s$ - $p$  perturbed scattered states (SK problem).

#### C. Local density of states of the perturbed system and extended Friedel sum rule

First we consider the various contributions to the local density of states at the rare-earth impurity site.

From (3.11) one has, similarly to (3.3),

$$\tilde{g}_{00}^{cc}(\omega) = \tilde{F}_{c,o}^R(\omega) - i\pi \tilde{\rho}_{c,o}(\omega), \quad (3.16)$$

where

$$\begin{aligned} \tilde{\rho}_{c,o}(\omega) &= -\frac{1}{\pi} \text{Im} \tilde{g}_{00}^{cc}(\omega) \\ &= \frac{\rho_c(\omega)}{[1 - V_{cc} F_c^R(\omega)]^2 + [\pi V_{cc} \rho_c(\omega)]^2} \end{aligned} \quad (3.17a)$$

is the local density of states of an  $s$ - $p$  subband in the SK problem,  $\tilde{F}_{c,o}^R(\omega)$  being given in terms of  $\rho_c(\omega)$  and  $F_c^R(\omega)$  as

$$\tilde{F}_{c,o}^R(\omega) = \frac{F_c^R(\omega)[1 - V_{cc}F_c^R(\omega)] - \pi^2 V_{cc}\rho_c^2(\omega)}{[1 - V_{cc}F_c^R(\omega)]^2 + [\pi V_{cc}\rho_c(\omega)]^2}. \quad (3.17b)$$

The total local density of states at the rare-earth impurity center is the sum of two contribu-

$$\rho_{d,o}(\omega) = -\frac{1}{\pi} \text{Im}G_{00}^{dd}(\omega) = |V_{cd}|^2 \frac{\tilde{\rho}_{c,o}(\omega)}{[\omega - \epsilon_d - |V_{cd}|^2 \tilde{F}_{c,o}^R(\omega)]^2 + [\pi |V_{cd}|^2 \tilde{\rho}_{c,o}(\omega)]^2} \quad (3.19)$$

is the local  $d$ -hump density of states and

$$\begin{aligned} \tilde{\rho}_{c,o}(\omega) &= -\frac{1}{\pi} \text{Im}G_{00}^{cc}(\omega) \\ &= \frac{(\omega - \epsilon_d)^2 \tilde{\rho}_{c,o}(\omega)}{[\omega - \epsilon_d - |V_{cd}|^2 \tilde{F}_{c,o}^R(\omega)]^2 + [\pi |V_{cd}|^2 \tilde{\rho}_{c,o}(\omega)]^2} \end{aligned} \quad (3.20)$$

is the local  $s$ - $p$  density of states for a given sub-band.

We close this paragraph deriving an extended Friedel theorem connecting the total change in density of states due to the AM resonance to the total change in the number of conduction states introduced by the AM resonance. In particular, the sum rule previously announced in (2.7) follows straightforwardly from the theorem.

From (3.13) and (3.14) one obtains for the change in the number of  $s$ - $p$  conduction states up to energy  $\omega$  introduced by the AM resonance:

$$\begin{aligned} \delta n^c(\omega) &= -\frac{1}{\pi} \text{Im} \int_{E_b}^{\omega} \sum_i [G_{ii}^{cc}(\omega') - \tilde{g}_{ii}^{cc}(\omega')] d\omega' \\ &= -\frac{1}{\pi} \text{Im} \int_{E_b}^{\omega} \frac{-|V_{cd}|^2 \partial \tilde{F}_{c,o}^R(\omega') / \partial \omega'}{\omega' - \epsilon_d - |V_{cd}|^2 \tilde{F}_{c,o}^R(\omega')} d\omega'. \end{aligned} \quad (3.21a)$$

The above expression may be rewritten

$$\begin{aligned} \delta n^c(\omega) &= -\frac{1}{\pi} \text{Im} \left( \int_{E_b}^{\omega} \frac{1 - |V_{cd}|^2 \partial \tilde{F}_{c,o}^R(\omega') / \partial \omega'}{\omega' - \epsilon_d - |V_{cd}|^2 \tilde{F}_{c,o}^R(\omega')} d\omega' \right. \\ &\quad \left. - \int_{E_b}^{\omega} \frac{d\omega'}{\omega' - \epsilon_d - |V_{cd}|^2 \tilde{F}_{c,o}^R(\omega')} \right) \\ &= -\frac{1}{\pi} \int_{E_b}^{\omega} \frac{\partial}{\partial \omega'} \text{Im} \ln [\omega' - \epsilon_d - |V_{cd}|^2 \\ &\quad \times \tilde{F}_{c,o}^R(\omega')] d\omega' - \delta n^d(\omega), \end{aligned} \quad (3.21b)$$

where  $\delta n^d(\omega)$  is the number of  $d$  states contained in the  $d$  hump up to energy  $\omega$  as follows from (3.10).

Then the total number of states introduced by the AM resonance  $\Delta Z_d(\omega) = \delta n^c(\omega) + \delta n^d(\omega)$  is connected to the total change in density of states  $\Delta \rho_{\text{tot}}(\omega)$  by

tions, which are obtained from  $G_{00}^{dd}(\omega)$  and  $G_{00}^{cc}(\omega)$ . One has

$$\rho_{\text{loc}}(\omega) = \rho_{d,o}(\omega) + \tilde{\rho}_{c,o}(\omega), \quad (3.18)$$

where

$$\begin{aligned} \Delta Z_d(\omega) &= \int_{E_b}^{\omega} \Delta \rho_{\text{tot}}(\omega') d\omega' \\ &= -\frac{10}{\pi} \int_{E_b}^{\omega} \frac{\partial}{\partial \omega'} \text{Im} \ln [\omega' - \epsilon_d - |V_{cd}|^2 \\ &\quad \times \tilde{F}_{c,o}^R(\omega')] d\omega' \\ &= \frac{10}{\pi} \int_{E_b}^{\omega} \frac{\partial}{\partial \omega'} \eta(\omega') d\omega', \end{aligned} \quad (3.22)$$

where the phase shift  $\eta(\omega)$  is given by

$$\eta(\omega) = \arctan \frac{\pi |V_{cd}|^2 \tilde{\rho}_{c,o}(\omega)}{\omega - \epsilon_d - |V_{cd}|^2 \tilde{F}_{c,o}^R(\omega)}. \quad (3.23)$$

The factor 10 in (3.22) accounts for the degeneracy of the  $d$  level with same spirit that degeneracy of the  $s$ - $p$  band was included in (2.4) through the factor 8.

Friedel's sum rule (2.7) follows directly from (3.22) by taking  $\omega = \epsilon_F$  and  $\Delta Z_d(\epsilon_F) = \Delta Z_d$ .

#### D. Spin polarization at the impurity site: Self-polarization hyperfine field

We consider now the Dyson-like equation (3.8) to evaluate the Green's-function matrix elements  $\Gamma_{00\sigma}^{\lambda\lambda}(\omega)$  ( $\lambda = c$  or  $d$ ). We calculate these matrix elements up to first order in the local exchange fields  $V_{\text{exch}}^{(\lambda)} = -\frac{1}{2} \sigma J^{(\lambda)} \langle S^z \rangle$ . Then we collect the spin-dependent terms, thus obtaining the local magnetizations  $m^{(\lambda)}(0)$  ( $\lambda = c$  or  $d$ ).

Within this Born approximation the Green's function matrix elements  $\Gamma_{ii\sigma}^{\lambda\lambda}(\omega)$  turn out to be

$$\begin{aligned} \Gamma_{ii\sigma}^{\lambda\lambda}(\omega) &= G_{ii}^{\lambda\lambda}(\omega) - \frac{1}{2} \sigma G_{i0}^{\lambda\lambda}(\omega) J^{(\lambda)} \langle S^z \rangle G_{i0}^{\lambda\lambda}(\omega) \\ &\quad - \frac{1}{2} \sigma G_{i0}^{\lambda\mu}(\omega) J^{(\mu)} \langle S^z \rangle G_{0i}^{\mu\lambda}(\omega) \\ &= G_{ii}^{\lambda\lambda}(\omega) + \delta \Gamma_{ii\sigma}^{\lambda\lambda}(\omega) \quad (\lambda, \mu = c \text{ or } d; \mu \neq \lambda). \end{aligned} \quad (3.24)$$

Using the previously obtained expressions for the spin-independent Green's functions  $G^{\lambda\mu}(\omega)$  ( $\lambda, \mu = c$  or  $d$ ) one finds after a little algebra

$$\begin{aligned} \delta\Gamma_{00}^{cc}(\omega) &= -\frac{\sigma}{2} J^{(c)} \langle S^z \rangle \frac{(\omega - \epsilon_d)^2 [\tilde{F}_{c,o}(\omega)]^2}{[\omega - \epsilon_d - |V_{cd}|^2 \tilde{F}_{c,o}(\omega)]^2} \\ &\quad - \frac{\sigma}{2} J^{(d)} \langle S^z \rangle \frac{|V_{cd}|^2 [\tilde{F}_{c,o}(\omega)]^2}{[\omega - \epsilon_d - |V_{cd}|^2 \tilde{F}_{c,o}(\omega)]^2} \end{aligned} \quad (3.25)$$

and

$$\begin{aligned} \delta\Gamma_{00}^{dd}(\omega) &= -\frac{\sigma}{2} J^{(d)} \langle S^z \rangle \frac{1}{[\omega - \epsilon_d - |V_{cd}|^2 \tilde{F}_{c,o}(\omega)]^2} \\ &\quad - \frac{\sigma}{2} J^{(c)} \langle S^z \rangle \frac{|V_{cd}|^2 [\tilde{F}_{c,o}(\omega)]^2}{[\omega - \epsilon_d - |V_{cd}|^2 \tilde{F}_{c,o}(\omega)]^2}. \end{aligned} \quad (3.26)$$

Then one obtains the local magnetizations  $m^{(\lambda)}(0)$ , by remembering that

$$m^{(\lambda)}(0) = -\frac{1}{\pi} \text{Im} \int_{E_b}^{\epsilon_F} \sum_{\sigma} [\sigma \delta \Gamma_{00\sigma}^{\lambda\lambda}(\omega)] d\omega \quad (3.27)$$

( $\lambda = c$  or  $d$ ).

Let us introduce now the local magnetic susceptibilities  $\chi^{\lambda\mu}(0)$  ( $\lambda, \mu = c$  or  $d$ ), which are the local magnetic responses of  $\lambda$  electrons to an "effective magnetic field" acting on  $\mu$  electrons. (In our case the "effective magnetic field" is supplied by the local exchange field  $V_{\text{exch}}^{(\lambda)}$ .) One has

(i) the  $c$ - $c$  local susceptibility  $\chi^{cc}(0)$ ,

$$\begin{aligned} \chi^{cc}(0) &= -\frac{1}{\pi} \text{Im} \int_{E_b}^{\epsilon_F} d\omega \frac{(\omega - \epsilon_d)^2 [\tilde{F}_{c,o}(\omega)]^2}{[\omega - \epsilon_d - |V_{cd}|^2 \tilde{F}_{c,o}(\omega)]^2} \\ &= -\frac{1}{\pi} \int_{E_b}^{\epsilon_F} d\omega \frac{(\omega - \epsilon_d)^2 [\tilde{F}_{c,o}(\omega)]^2}{[\omega - \epsilon_d - |V_{cd}|^2 \tilde{F}_{c,o}(\omega)]^2} \\ &\quad \times \sin[2\eta(\omega) - 2\delta_c(\omega)]; \end{aligned} \quad (3.28a)$$

(ii) the "cross" local susceptibility  $\chi^{\text{mix}}(0)$ ,

$$\begin{aligned} \chi^{\text{mix}}(0) &= \chi^{cd}(0) = \chi^{dc}(0) \\ &= -\frac{1}{\pi} \text{Im} \int_{E_b}^{\epsilon_F} d\omega \frac{|V_{cd}|^2 [\tilde{F}_{c,o}(\omega)]^2}{[\omega - \epsilon_d - |V_{cd}|^2 \tilde{F}_{c,o}(\omega)]^2} \\ &= \frac{1}{\pi} \int_{E_b}^{\epsilon_F} d\omega \frac{|V_{cd}|^2 [\tilde{F}_{c,o}(\omega)]^2}{|X(\omega)|^2} \\ &\quad \times \sin[2\eta(\omega) - 2\delta_c(\omega)]; \end{aligned} \quad (3.28b)$$

and (iii) the  $d$ - $d$  local susceptibility  $\chi^{dd}(0)$ ,

$$\begin{aligned} \chi^{dd}(0) &= -\frac{1}{\pi} \text{Im} \int_{E_b}^{\epsilon_F} \frac{d\omega}{[\omega - \epsilon_d - |V_{cd}|^2 \tilde{F}_{c,o}(\omega)]^2} \\ &= \frac{1}{\pi} \int_{E_b}^{\epsilon_F} d\omega \frac{\sin[2\eta(\omega)]}{|X(\omega)|^2}. \end{aligned} \quad (3.28c)$$

$\eta(\omega)$  is given by (3.23), whereas the quantities  $|X(\omega)|$ ,  $|\tilde{F}_{c,o}(\omega)|$ , and  $\delta_c(\omega)$  are defined by

$$X(\omega) = \omega - \epsilon_d - |V_{cd}|^2 \tilde{F}_{c,o}(\omega) = |X(\omega)| e^{-i\eta(\omega)}, \quad (3.29a)$$

with

$$|X(\omega)| = \{[\omega - \epsilon_d - |V_{cd}|^2 \tilde{F}_{c,o}^R(\omega)]^2 + [\pi |V_{cd}|^2 \tilde{\rho}_{c,o}(\omega)]^2\}^{1/2} \quad (3.29b)$$

and

$$\tilde{F}_{c,o}(\omega) = |\tilde{F}_{c,o}(\omega)| e^{-i\delta_c(\omega)}, \quad (3.30a)$$

with

$$|\tilde{F}_{c,o}(\omega)| = \{[\tilde{F}_{c,o}^R(\omega)]^2 + [\pi \tilde{\rho}_{c,o}(\omega)]^2\}^{1/2}, \quad (3.30b)$$

$$\delta_c(\omega) = \arctan[\pi \tilde{\rho}_{c,o}(\omega) / \tilde{F}_{c,o}^R(\omega)]. \quad (3.30c)$$

The contribution to the local magnetization due to one conduction  $s$ - $p$  subband is

$$\begin{aligned} m^{(c)}(0) &= J^{(c)} \langle S^z \rangle \chi^{cc}(0) + 5 J^{(d)} \langle S^z \rangle \chi^{\text{mix}}(0) \\ &= J^{(c)} \langle S^z \rangle \left( 1 + 5 \frac{J^{(d)}}{J^{(c)}} \frac{\chi^{\text{mix}}(0)}{\chi^{cc}(0)} \right) \chi^{cc}(0) \\ &= J^{(c)} \langle S^z \rangle \tilde{\chi}^{cc}(0). \end{aligned} \quad (3.31)$$

The inclusion of the factor 5 in (3.31) is because one has five different scattering channels whereby a conduction electron in a given  $s$ - $p$  subband can be admixed into an AM  $d$  resonance and go back to the  $s$ - $p$  subband. The local magnetization due to a  $d$  hump is

$$\begin{aligned} m^{(d)}(0) &= J^{(d)} \langle S^z \rangle \chi^{dd}(0) + J^{(c)} \langle S^z \rangle \chi^{\text{mix}}(0) \\ &= J^{(d)} \langle S^z \rangle \chi^{dd}(0) \left( 1 + \frac{J^{(c)}}{J^{(d)}} \frac{\chi^{\text{mix}}(0)}{\chi^{dd}(0)} \right) \\ &= J^{(d)} \langle S^z \rangle \tilde{\chi}^{dd}(0). \end{aligned} \quad (3.32)$$

So, the total magnetization at the impurity center is

$$m(0) = 4m^{(c)}(0) + 5m^{(d)}(0) \quad (3.33)$$

Until now the  $s$  and  $p$  conduction states have played the same role in the above calculations. In fact, within our model, they are indistinguishable in several steps of the computation, namely, that of the charge perturbations affecting the conduction band, of the self-consistent position of the virtual  $d$ -level  $\epsilon_d$  in the conduction band and in the  $|V_{cd}|^2$  phenomenological parameter responsible for the broadening of the virtual bound state.

However, in order to compute the self-polarization hyperfine field, one must consider  $s$  and  $p$  electrons as contributing differently to the hyperfine field. We have the following contributions to the hyperfine field:

$$H_{\text{hf}}^{(\text{tot})} = H_{\text{hf}}^{(s)} + H_{\text{hf}}^{(p)} + H_{\text{hf}}^{(d)}, \quad (3.34)$$

where

$$H_{\text{hf}}^{(d)} = -5 A_{\text{cp}}^{(d)} m^{(d)}(0), \quad (3.35)$$

$A_{\text{cp}}^{(d)}$  being the hyperfine  $d$ -core polarization parameter and the factor 5 accounting for degeneracy of

the  $d$  levels.

The  $s$  and  $p$  contributions to the hyperfine field, given, respectively, by  $H_{\text{hf}}^{(s)}$  and  $H_{\text{hf}}^{(p)}$  are to be computed from

$$H_{\text{hf}}^{(s)} = A(Z) m^{(s)}(0) \quad (3.36a)$$

and

$$H_{\text{hf}}^{(p)} = -A_{\text{cp}}^{(p)} m^{(p)}(0), \quad (3.36b)$$

where  $A(Z)$  is the "true" Fermi contact interaction and  $A_{\text{cp}}^{(p)}$  is the  $p$  induced core polarization. We compute here, consistently with the assumption of the uniform distribution of  $s$ - $p$  states,  $m^{(s)}(0)$  and  $m^{(p)}(0)$  as

$$m^{(s)}(0) = m^{(c)}(0), \quad (3.37a)$$

$$m^{(p)}(0) = 3m^{(c)}(0). \quad (3.37b)$$

So, one has

$$H_{\text{hf}}^{(s)} + H_{\text{hf}}^{(p)} = H_{\text{hf}}^{(c)} = A_{\text{eff}}(Z) m^{(c)}(0), \quad (3.38a)$$

with

$$A_{\text{eff}}(Z) = A(Z) - 3A_{\text{cp}}^{(p)}, \quad (3.38b)$$

and the total hyperfine field may be written in final form as

$$H_{\text{hf}}^{(\text{tot})} = A_{\text{eff}}(Z) m^{(c)}(0) - 5A_{\text{cp}}^{(d)} m^{(d)}(0). \quad (3.39)$$

The simplified band structure picture adopted implies a certain effective Fermi contact interaction which includes corrections from the  $p$ -induced core polarization, as seen from (3.38b). This is perhaps at the origin of Campbell's<sup>16</sup> almost perfect fitting of the hyperfine field of  $s$ - $p$  impurities in ferromagnetic host using the simple Fermi-Segrè formula for the contact interaction, because of a subtle compensation of pure  $s$  and  $p$  contributions to the hyperfine constant. So, we adopt in this work (cf. Sec. IV B) the estimate by Campbell of  $A_{\text{eff}}(Z)$ .

#### IV. NUMERICAL RESULTS

We divide this section in two subsections. Section IV A is devoted to illustrate some consequences of the theoretical approach presented in Sec. III. Since some unfamiliar features are associated to the strong scattering which is present in the SK problem, we discuss in detail certain points which reflect the deviations from the classical AM results. In Sec. IV B we discuss the behavior of the hyperfine field.

The numerical calculations are performed for a simplified band-structure model. Each pure host  $s$ - $p$  subband is described by a "parabolic"-like density of states<sup>14</sup>:

$$\rho_c(\omega) = \begin{cases} \frac{3}{4\Delta_c} \left[ 1 - \left( \frac{\omega}{\Delta_c} \right)^2 \right], & E_b < \omega < E_t \\ 0, & \text{otherwise,} \end{cases} \quad (4.1)$$

where  $\Delta_c$  is the half width of the subband so that

$$\int_{E_b}^{E_t} \rho_c(\omega) d\omega = 1.$$

We hope that this example will be useful to give an insight on the whole problem, but indeed some effects related to the details of actual  $s$ - $p$  band structures cannot be accounted for properly. However, since  $\rho_c(\omega)$  is an entry quantity in our formulation all the required features which could be obtained using sophisticated band calculations for the description of the density of states of real  $s$ - $p$  bands can be naturally incorporated in our formulation, together with straightforward embellishments of our model.

##### A. Some consequences of the theoretical model

In Fig. 1 we plot as a function of the energy  $\omega$  the phase shifts  $\eta(\omega)$  given by (3.23). The energy varies from the bottom to the top of the conduction subband. These phase shifts are plotted for the following choice of parameters: (i) the  $|V_{cd}|^2$  mixing parameter, which is a phenomenological one. We take always in Fig. 1,  $|V_{cd}|^2 = 0.1$ ; (ii) the position of the  $d$  bound state level, which may take values between  $E_b$  and  $E_t$ ; and (iii) the perturbative  $V_{cc}$  charge potential; this is a repulsive potential and two kinds of regimes occur. (a) When  $V_{cc}$  is less than  $V_{cc}^{\text{crit}}$ , ( $V_{cc}^{\text{crit}} = [F_c^R(E_t)]^{-1}$  being the potential to repel a bound state above the top of the subband), a "piling up" of states in the region near the top of the subband is observed. For the band shape (4.1) one has  $V_{cc}^{\text{crit}} = 0.667$ . (b) After a bound state is repelled the number of extended states decreases and consequently the previously (SK) strongly perturbed Moriya band becomes flatter and flatter.

In Fig. 1(a) we show the phase shift for  $\epsilon_d = 0$ ,  $V_{cc}$  spanning the two above-mentioned regimes. For  $V_{cc} = 0$  the usual symmetric AM behavior is recovered, whereas for strongly repulsive limits ( $V_{cc} = 0.8$  and  $V_{cc} = 1.0$ ) the classical behavior defined by a steep increase of  $\eta(\omega)$  around  $\epsilon_d$  is obtained. This is easily understood since the perturbed density of states is rather small and flat. To emphasize the consequences of the strong perturbation regime ( $V_{cc} > V_{cc}^{\text{crit}}$ ) we plot in Fig. 1(b), for  $V_{cc} = 0.8$ ,  $\eta(\omega)$  for some values of  $\epsilon_d$ . The same kind of behavior obtained for  $\epsilon_d = 0$  is observed here for  $\epsilon_d = -0.4$  and  $\epsilon_d = 0.4$  although there exists a tendency to flatten the change in slope of  $\eta(\omega)$  as one goes from  $E_b$  to  $E_t$ . This is related to a smooth increase with energy of the perturbed density of

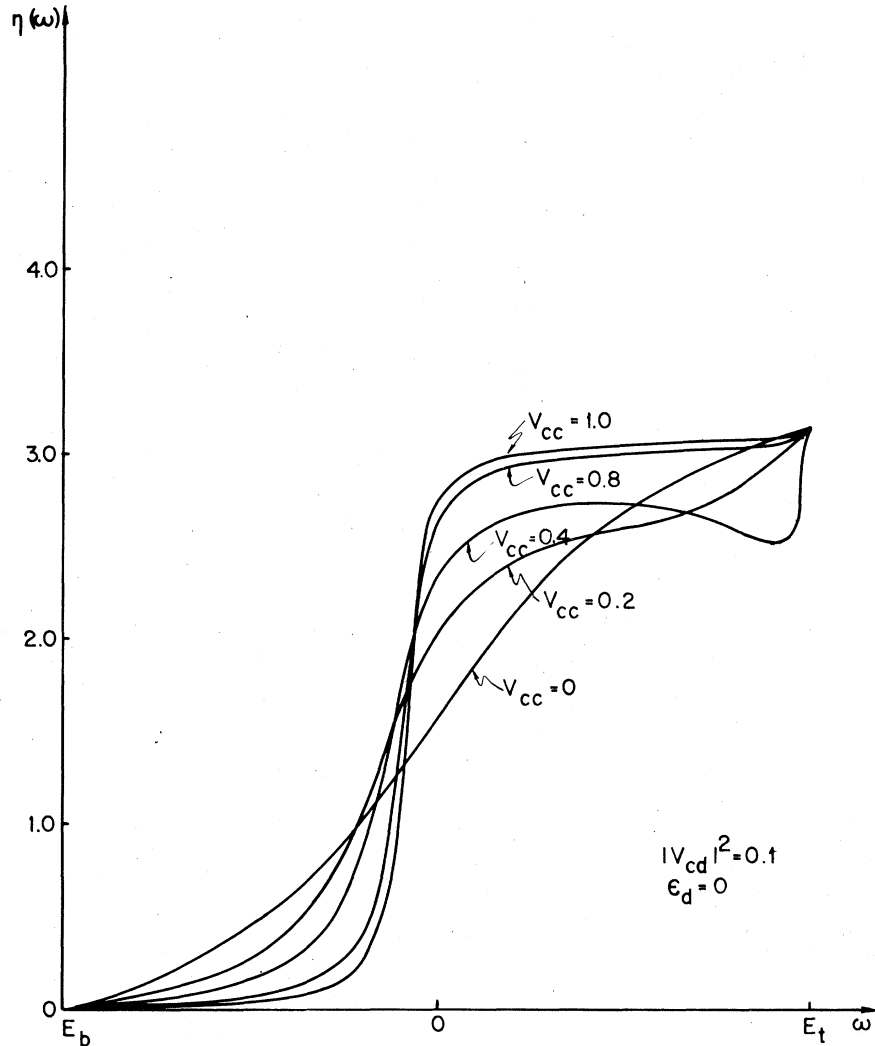


FIG. 1. Phase shifts  $\eta(\omega)$  as a function of energy for the band model (4.1). (a)  $\epsilon_d = 0$  and several values for the SK potential. Values of  $V_{cc}$  larger and smaller than  $V_{cc}^{\text{crit}}$  are used. (b) Several values of  $\epsilon_d$  and the SK potential is taken  $V_{cc} = 0.8 > V_{cc}^{\text{crit}}$ . (c) Several values of  $\epsilon_d$  and the SK potential is taken  $V_{cc} = 0.4 < V_{cc}^{\text{crit}}$ .

states. This behavior illustrates small departures from a flat density of states, reflecting an increasingly smooth variation of  $\eta(\omega)$  with energy. Next we return to Fig. 1(a) to discuss the "piling up" regime ( $0 < V_{cc} < V_{cc}^{\text{crit}}$ ). For energies near  $E_t$ ,  $\eta(\omega)$ , which showed a monotonic increase towards  $\pi$  for both cases  $V_{cc} = 0$  and  $V_{cc} > V_{cc}^{\text{crit}}$ , now decreases to give rise finally to a rapid increase to  $\pi$ .

In order to investigate the origin of this behavior and its connection to the SK problem we show in Fig. 1(c)  $\eta(\omega)$  for  $V_{cc} = 0.4$  and for several values of  $\epsilon_d$ . We plot also in Fig. 1(c),  $|V_{cd}|^2 \bar{F}_{c,0}^R(\omega)$  as a function of  $\omega$ . Comparing to the unperturbed result ( $V_{cc} = 0$ ) one verifies that the Hilbert transform which is perfectly symmetric and small for  $V_{cc} = 0$  becomes highly asymmetric for a strong piling up of states near  $E_t$ . This effect is typical of  $V_{cc}$  close to the condition for repelling a bound

state from the band and is to be contrasted to the strong perturbation regime where the Hilbert transforms take only small values (negative and positive) along the band.

To discuss the unfamiliar behavior we obtain for  $\eta(\omega)$  we analyze the denominator  $X(\omega) = \omega - \epsilon_d - |V_{cd}|^2 \bar{F}_{c,0}^R(\omega)$ , which appears in the definition of  $\eta(\omega)$  [cf. (3.23)]. The zeros of that function give the energies at which the phase shift passes through  $\pi/2$ . In the top of Fig. 1(c) the straight lines  $\omega - \epsilon_d$  determine the energy values for which  $\eta(\omega) = \pi/2$ . Since both plots in Fig. 1(c) are in the same scale we have marked a cross in the corresponding energies for  $\eta(\omega)$ . Depending on the values of  $\epsilon_d$  one sees that the straight lines cross  $|V_{cd}|^2 \bar{F}_{c,0}^R(\omega)$  one or three times and the last situation is at the origin of the anomalous behavior of  $\eta(\omega)$ .

We stress that these strong deviations from the AM results are a direct consequence of the defor-

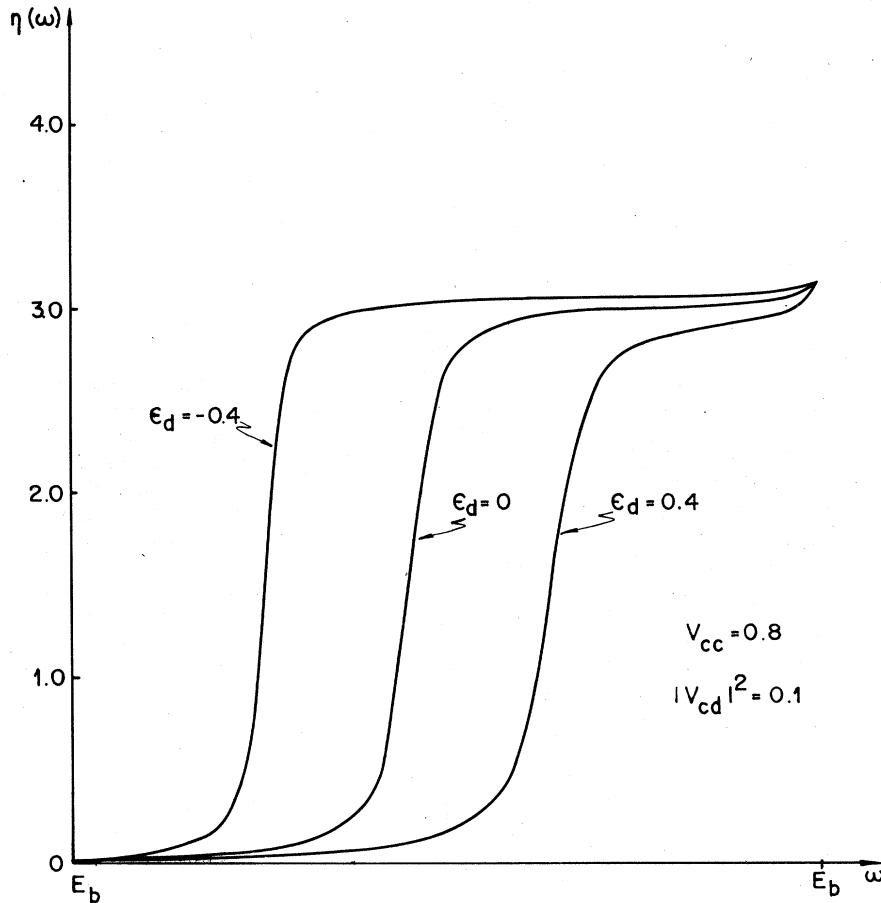


Fig. 1. (Continued)

mations of the density of states. In our case these are SK induced deformations but a quite similar behavior would be observed for a band model exhibiting a peak in the high-energy region. These features however depend on the choice of  $|V_{cd}|^2$ . In fact, if one reduces its value, the curve  $|V_{cd}|^2 \tilde{F}_{c,0}^R(\omega)$  of the top of Fig. 1(c) is rescaled and these unfamiliar effects are wiped out.

Figure 2 describes the local  $d$ -hump density of states  $\rho_{d,0}(\omega)$  as a function of the energy for different band fillings, i.e.,  $Z_h$  varying from 2 to 7. We have taken for  $|V_{cd}|^2$  the values 0.05 [Fig. 2(a)] and 0.1 [Fig. 2(b)], respectively. We consider that the trivalent rare-earth impurity contributes one electron to the  $d$  hump ( $Z_{\text{imp}}^{(d)} = 1$ ), the remaining ones being associated with the  $s$ - $p$  conduction states. The dotted points correspond to the values of the Fermi energy associated to each value of  $Z_h$ . These self-consistent results are obtained by imposing in the extended Friedel sum rule (2.7) an occupation number of one electron for the  $d$ -hump state.

In Fig. 2(a) the self-consistently calculated  $d$ -hump density of states exhibits only weak distur-

tions. This is to be compared to Fig. 2(b) where for intermediate occupations strong distortions occur, these distortions being related to the above-discussed unfamiliar behavior of  $\eta(\omega)$ . Note that in  $\eta(\omega)$  are included both  $d$ -hump and extended-state contributions [cf. (3.22)]. From Fig. 2 one observes a  $d$ -state contribution (which is positive) at the high-energy part of the band. So, the difference  $\partial \eta(\omega) / \partial \omega - \rho_{d,0}(\omega)$  gives a measure of the strong deviations from the result of the Anderson-Clogston compensation theorem<sup>19</sup> due to the highly nonflat density of states.

Figure 3 illustrates, for  $V_{cc} = 0.2$ , the expressions (3.19), (3.17a), and (3.20) obtained in Sec. III for the local densities of states, namely:  $d$  hump (dotted lines), SK density of states (dot-trace curve), and the  $|V_{cd}|^2$  perturbed AM local conduction density of states. A hybridization induced depression on the SK density of states is clearly shown: in particular for  $\omega = \epsilon_d$  the local conduction density of states vanishes. The negative change associated to the depression may overcome the positive one associated to the  $d$ -hump and therefore  $\partial \eta(\omega) / \partial \omega$  becomes negative

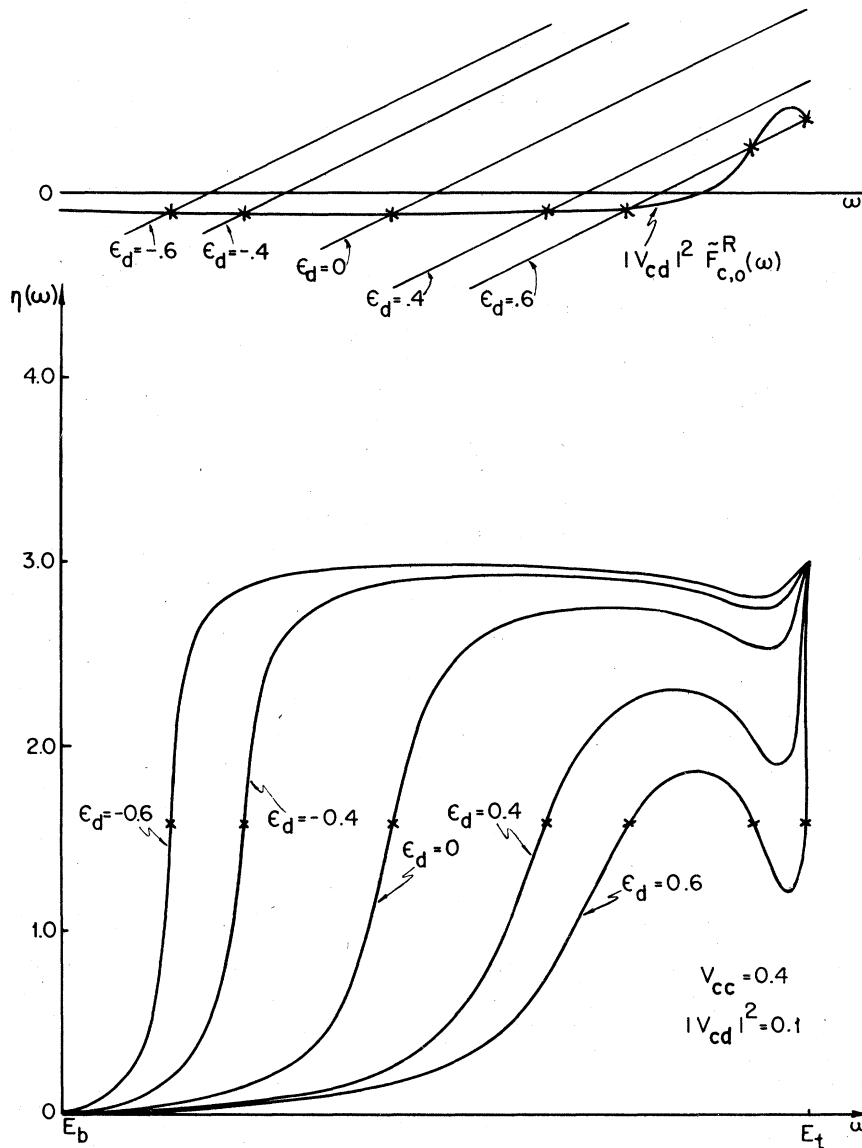


Fig. 1. (Continued)

as reflected in the phase shift plots.

Next we report in Figs. 4-6 the results obtained for the local magnetic responses  $\chi^{dd}(0)$ ,  $\chi^{cc}(0)$  and  $\chi^{\text{mix}}(0)$  [cf. (3.28)]. The dotted lines joining the crosses indicate the self-consistent values of  $\chi^{dd}(0)$ ,  $\chi^{cc}(0)$ , and  $\chi^{\text{mix}}(0)$  for several hosts.

Figure 4 shows that  $\chi^{dd}(0)$  has the same characteristics of the AM-like  $d$  density of states, i.e., an asymmetry of the shape of the local magnetic response coherently with the deformation of the  $d$ -hump states. An interesting feature of Fig. 4 concerns the strongly deformed magnetic responses associated with the strong perturbed SK problem. In Fig. 4(a) this corresponds to  $Z_h=4, 5, \text{ and } 6$ . In this case the self-consistently determined  $V_{cc}$  correspond to values around the

critical one to extract the bound state. Again the behavior reflects a feature of the piling up regime. Similarly to  $\rho_{d,0}(\omega)$ , a reduction of  $|V_{cd}|^2$  wipes out these effects as shown in Fig. 4(b).

$\chi^{cc}(0)$  is plotted in Fig. 5 for  $|V_{cd}|^2=0.05$ . A general characteristic of the curves  $\chi^{cc}(0)$  is the existence of a depression in the local  $c$ - $c$  response, precisely around the corresponding peak in  $\chi^{dd}(0)$  shown in Fig. 4 and a hump outside this region. For  $Z_h=2$  the SK potential vanishes and one obtains a symmetric curve for  $\chi^{cc}(0)$ . For increasing values of  $Z_h$  the asymmetry of  $\chi^{cc}(0)$  increases until one obtains a saturated regime where bound states are repelled from the band.

The cross magnetic response  $\chi^{\text{mix}}(0)$  is plotted in Fig. 6 for  $|V_{cd}|^2=0.05$ . One observes a change

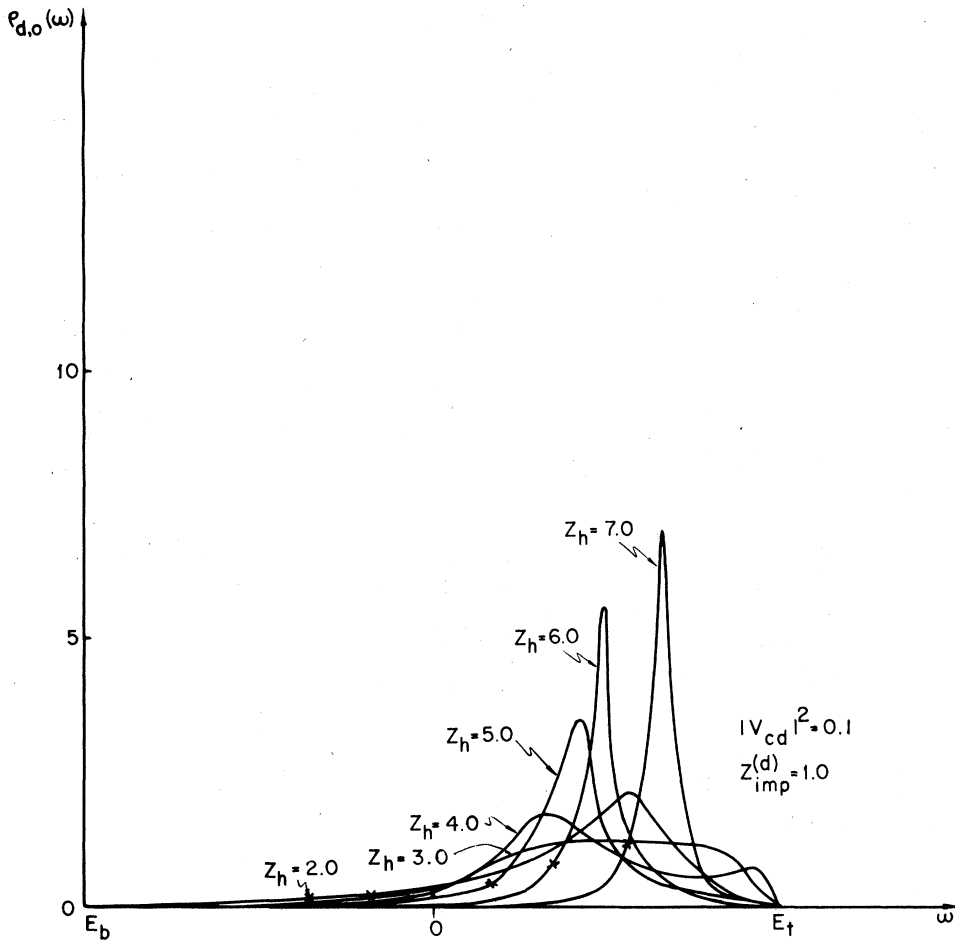


FIG. 2. Local  $d$  density of states self-consistently calculated for band fillings ranging from 2 to 7. (a)  $|V_{cd}|^2 = 0.1$ . (b)  $|V_{cd}|^2 = 0.05$ .

in sign in the local response and these changes correspond *grosso modo* to the depression region in  $\chi^{cc}(0)$  or to the peak in  $\chi^{dd}(0)$ . It should be stressed that for the adopted number of electrons in the resonant state the self-consistent values of  $\chi^{\text{mix}}(0)$  (dotted lines) are always positive.

#### B. Self-polarization hyperfine field

The theoretical results (3.35) and (3.38) for the self-polarization field involve the exchange parameters  $J^{(\lambda)}$ , the hyperfine couplings  $A_{\text{eff}}(Z)$  and  $A_{\text{cp}}^{(d)}$ , and the local magnetic responses  $\chi^{\lambda\mu}(0)$ .

In order to compare the theoretical results to experiments a brief account of the various contributions to the hyperfine field at the rare-earth impurity nucleus is worthwhile. The total field is given by the sum of three terms: the  $f$ -core hyperfine field, the self-polarization field (which is computed in this work), and the transferred field. An experimental procedure to extract from the data the relevant contribution to be compared with our predictions goes as follows. The  $f$ -core-state

contribution can be known from experiments in insulating matrices. On the other hand, consider small quantities of nonmagnetic elements like Lu in alloys such as  $(\text{Lu}_x\text{R}_{1-x})_y\text{M}_y$ ,  $R$  being the spin-carrying rare-earth element whereas  $M$  is the  $s$ - $p$  host. A measurement performed at the Lu site "sees" directly the transferred hyperfine field. Then the self-polarization field can be obtained.

Throughout this work,  $J^{(\lambda)}$  is assumed to be independent of  $k$  and  $q$ . This enables us to obtain the self-polarization field as a function of the local magnetic responses  $\chi^{\lambda\mu}(0)$ , which incorporate the impurity effects. Otherwise, if one considers  $J^{(\lambda)}(\vec{k} + \vec{q}, \vec{k})$  one has to compute numerically the impurity perturbed magnetic responses  $\chi^{\lambda\mu}(\vec{k} + \vec{q}, \vec{k})$  which involve complicated sums over the Brillouin zone. Even in the assumption of  $J^{(\lambda)}$  independent of  $\vec{k}$  and  $\vec{q}$ , the transferred field would be extremely difficult to calculate theoretically since it still involves the calculation of magnetic susceptibilities which are  $\vec{k}, \vec{q}$  dependent. In this way, the above suggested experimental technique would circumvent this difficulty.

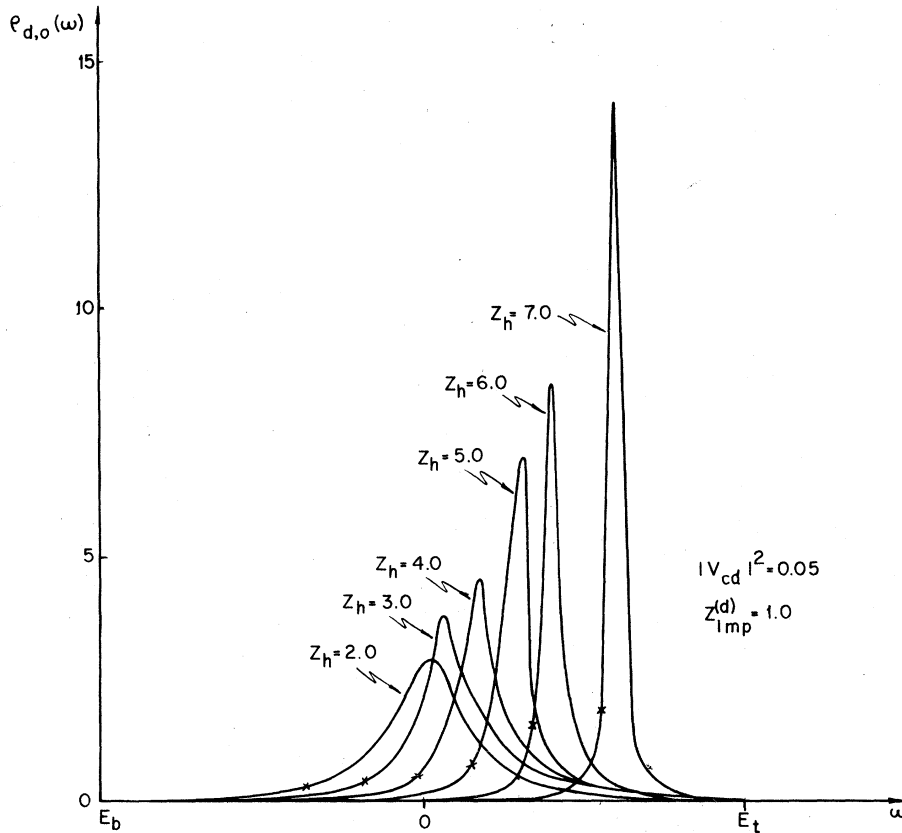


Fig. 2. (Continued)

The values of  $J^{(d)}$  and  $J^{(c)}$  can be extracted from "atomiclike" calculations.<sup>20</sup> In absolute value the ratio  $J^{(d)}/J^{(c)}$  ranges between 1 and 2.

In the present work, contrary to the case of transition metal hosts<sup>6</sup> the sign of  $J^{(d)}$  is always positive. This is because no available next-neighbor impurity  $d$  sites are expected to be present in  $s$ - $p$  (or noble) hosts, thus inhibiting a possible direct  $d$ - $f$  Heisenberg-like exchange between next neighbor  $d$  and  $f$  orbitals. Within our model of eight identical  $s$ - $p$  conduction subbands, the effective exchange coupling  $J^{(c)}$  [similarly to  $A_{\text{eff}}(Z)$  defined in (3.38b)] is given by  $J^{(c)} = J^{(s)} + 3J^{(p)}$ .

Actually,  $J^{(p)}$  would eventually be negative (due to a direct  $p$ - $f$  Heisenberg exchange) and overcome the pure positive  $s$  contribution.

Furthermore the hyperfine couplings can be only crudely estimated.<sup>16</sup> So we intend to rewrite (3.35) and (3.38) in such a way that only ratios  $A_{\text{cp}}^{(d)}/A_{\text{eff}}(Z)$  appear. As a consequence the contact and  $d$ -induced core contributions to the self-polarization field are given in units of  $J^{(c)}A_{\text{eff}}(Z)\langle S^z \rangle$  and the exchange parameters appear also as the ratio  $J^{(d)}/J^{(c)}$ . One has

$$\frac{H_{\text{hf}}^{(c)}}{J^{(c)}A_{\text{eff}}(Z)\langle S^z \rangle} \tilde{\chi}^{cc}(0) = \chi^{cc}(0) \left( 1 + 5 \frac{J^{(d)}}{J^{(c)}} \frac{\chi^{\text{mix}}(0)}{\chi^{cc}(0)} \right) \quad (4.2)$$

and

$$\begin{aligned} \frac{H_{\text{hf}}^{(d)}}{J^{(c)}A_{\text{eff}}(Z)\langle S^z \rangle} &= -5 \frac{A_{\text{cp}}^{(d)}}{A_{\text{eff}}(Z)} \frac{J^{(d)}}{J^{(c)}} \tilde{\chi}^{da}(0) \\ &= -5 \frac{A_{\text{cp}}^{(d)}}{A_{\text{eff}}(Z)} \frac{J^{(d)}}{J^{(c)}} \chi^{da}(0) \\ &\quad \times \left( 1 + \frac{J^{(c)}}{J^{(d)}} \frac{\chi^{\text{mix}}(0)}{\chi^{da}(0)} \right). \end{aligned} \quad (4.3)$$

Since we consider the rare-earth nucleus, we use Campbell's estimate<sup>16</sup> of  $A_{\text{cp}}^{(d)}$  for  $5d$  states and  $A_{\text{eff}}(Z)$  appropriate of rare earths, the ratio  $A_{\text{cp}}^{(d)}/A_{\text{eff}}(Z)$  should be varied about  $\frac{1}{4}$ . The difficulties in estimating the ratios  $J^{(d)}/J^{(c)}$  and  $A_{\text{cp}}^{(d)}/A_{\text{eff}}(Z)$  are of different character. In fact, as mentioned before some estimates of  $J^{(d)}$  and  $J^{(c)}$  are available from plane-wave or atomic like calculations<sup>20</sup>; on the other hand, hyperfine coupling constants involve extremely delicate atomic calculations. In this way, within our theory, the

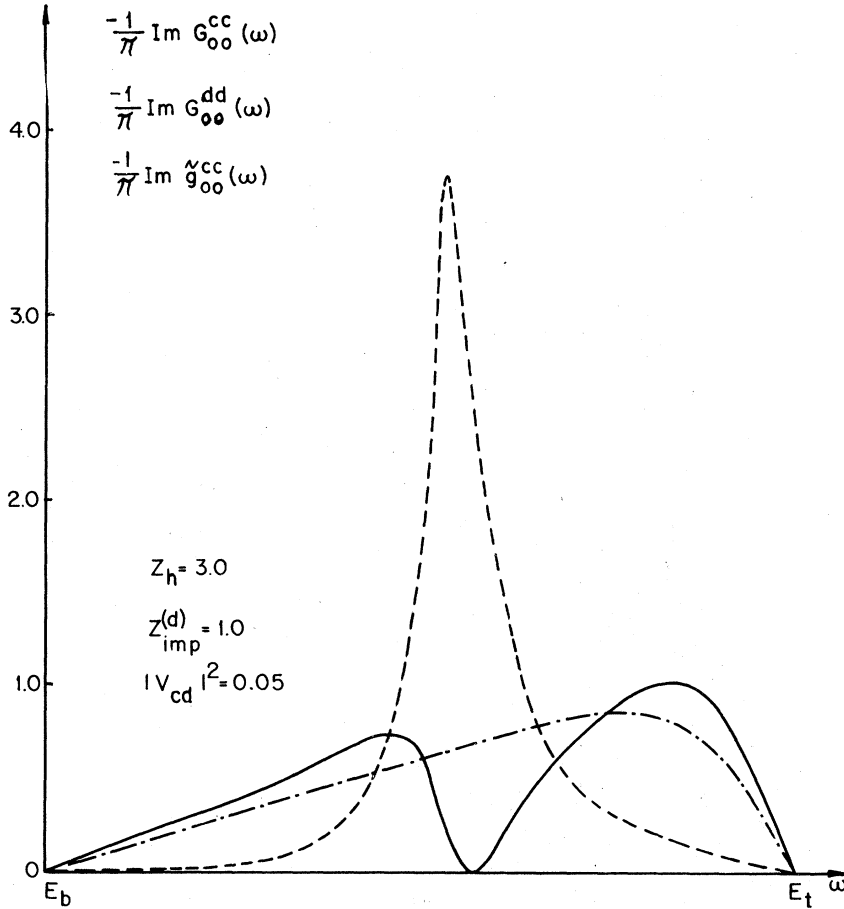


FIG. 3. Dot-dash line shows the SK perturbed local density of states for  $s$ - $p$  conduction states. The dotted line shows the  $d$ -hump density of states, whereas the full line shows the local density of states of the  $s$ - $p$  subband in presence of both SK and AM perturbations. These results are obtained for  $Z_h = 3$  and  $|V_{cd}|^2 = 0.05$ .

product  $(J^{(d)}/J^{(c)}) A_{cp}^{(d)}/A_{eff}(Z)$  may be taken as a flexible parameter which should be varied about the estimate<sup>16</sup>  $A_{cp}^{(d)}/A_{eff}(Z) = \frac{1}{4}$  and  $J^{(d)}/J^{(c)} = 2$ .<sup>20</sup>

Let us now propose some fundamental assumptions about the basis of the self-consistency procedure adopted in our calculations. The SK impurity problem is defined by the charge difference  $\Delta Z_c = Z_{imp}^{(c)} - Z_h$ . The number  $Z_{imp}^{(d)}$  specifies for trivalent rare earths, for instance, the number of electrons to be put in the AM  $d$  resonant state,  $Z_{imp}^{(d)} = 3 - Z_{imp}^{(c)}$ . Since the strength of the SK perturbation of the  $s$ - $p$  conduction states depends on the value of  $Z_{imp}^{(c)}$  for the number of electrons in a given host, the deformation of the AM resonance is a function of this SK perturbation. On the other hand, for a given value of  $Z_{imp}^{(c)}$  which determines the SK perturbation, the amount of occupied  $d$  states in the AM resonance depends strongly on the value of the phenomenological admixture parameter  $|V_{cd}|^2$ . In the numerical calculations throughout we consider  $Z_{imp}^{(c)} = 2$ , which corresponds to adopting the  $d$  occupancy equal to one electron

for a trivalent rare earth. With this choice the SK perturbation is defined for any host. The role of varying the  $d$ -state occupation with respect to the "ionic value" is ascribed to  $|V_{cd}|^2$ . In fact, due to the SK-induced strong deviations from the Anderson-Clogston theorem,<sup>19</sup> for a given  $|V_{cd}|^2$  the  $d$ -state occupation number may be quite different from 1. Furthermore, changing  $|V_{cd}|^2$ , we induce for a fixed SK perturbation a varying  $d$ -state occupation.

In Fig. 7 we plot the total and partial (contact and  $d$ -core induced) fields for several hosts as a function of the  $|V_{cd}|^2$  admixture parameter,  $A_{cp}^{(d)}/A_{eff}(Z)$  and  $J^{(d)}/J^{(c)}$  ( $J^{(c)} > 0$ ) being taken, respectively, as  $\frac{1}{4}$  and 2. In this figure the main tendencies predicted by our model are exhibited. For suitable ranges of  $|V_{cd}|^2$ , which controls the amount of  $d$ -like electrons in the AM hump, the total hyperfine field may change sign at the end of the series. This is because the increasing number of  $d$  electrons puts the Fermi energy level in a region of higher density of states, thus

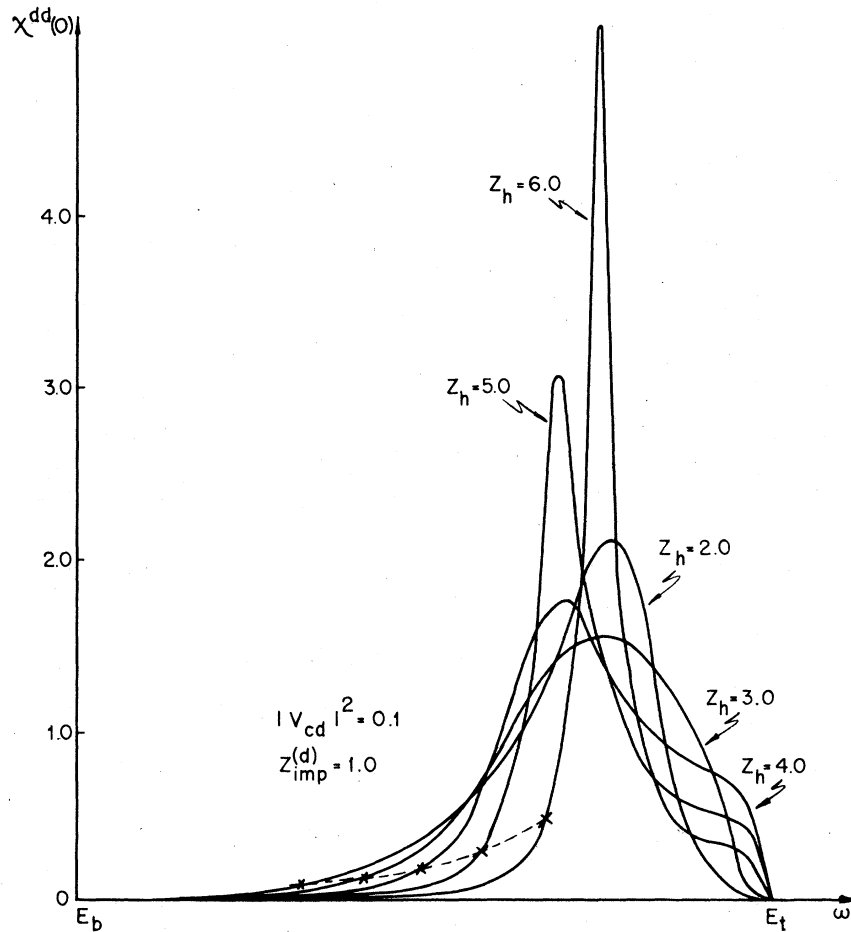


FIG. 4.  $d$ - $d$  local magnetic susceptibility  $\chi^{dd}(0)$  for the band model (4.1) as a function of energy. The dotted lines joining the crosses and the self-consistent values of  $\chi^{dd}(0)$  for several hosts. (a)  $|V_{cd}|^2 = 0.1$ . (b)  $|V_{cd}|^2 = 0.05$ .

increasing the  $d$ - $d$  local magnetic response and consequently the  $d$ -core polarization contribution which is negative (for  $J^{(d)} > 0$ ).

In Figs. 7(a)–7(c) we can follow how the  $d$ -core contribution decreases with increasing  $|V_{cd}|^2$ . To understand this we recall that in all these plots the SK impurity charge  $Z_{\text{imp}}^{(c)}$  is kept constant,  $Z_{\text{imp}}^{(c)} = 2$ . So, this change is ascribed to  $|V_{cd}|^2$ . The physical mechanism behind the decrease of the local  $d$ - $d$  susceptibility  $\chi^{dd}(0)$  can be seen through the self-consistently determined dotted lines in Figs. 4(a) and 4(b) for two different values of  $|V_{cd}|^2$ . However, from (4.3), the local pure  $d$ - $d$  response  $\chi^{dd}(0)$  is multiplied by a correction factor  $1 + (J^{(c)}/J^{(d)}) \chi^{\text{mix}}(0)/\chi^{dd}(0)$ . In Fig. 6 one sees that the self-consistent calculated  $\chi^{\text{mix}}(0)$  is al-

ways positive. We have numerically verified that the self-consistent  $\chi^{\text{mix}}(0)$  is roughly independent on the choice of  $|V_{cd}|^2$ . So, for a given positive ratio  $J^{(d)}/J^{(c)}$  the correction factor  $1 + (J^{(c)}/J^{(d)}) \chi^{\text{mix}}(0)/\chi^{dd}(0)$  decreases with decreasing  $|V_{cd}|^2$ . It turns out numerically that the  $d$ -core contribution to the hyperfine field, which is proportional to  $\tilde{\chi}^{dd}(0)$ , is dominated by the pure  $d$ - $d$  response  $\chi^{dd}(0)$ .

Concerning the behavior of the contact contribution to the hyperfine field, in this case the sign of  $J^{(d)}/J^{(c)}$  is extremely important in discussing the variation of the local magnetic response. In fact, Fig. 5 shows that the self-consistent value of  $\chi^{cc}(0)$  decreases when one goes from the beginning to the end of the series. Then, the ratio  $\chi^{\text{mix}}(0)/\chi^{cc}(0)$

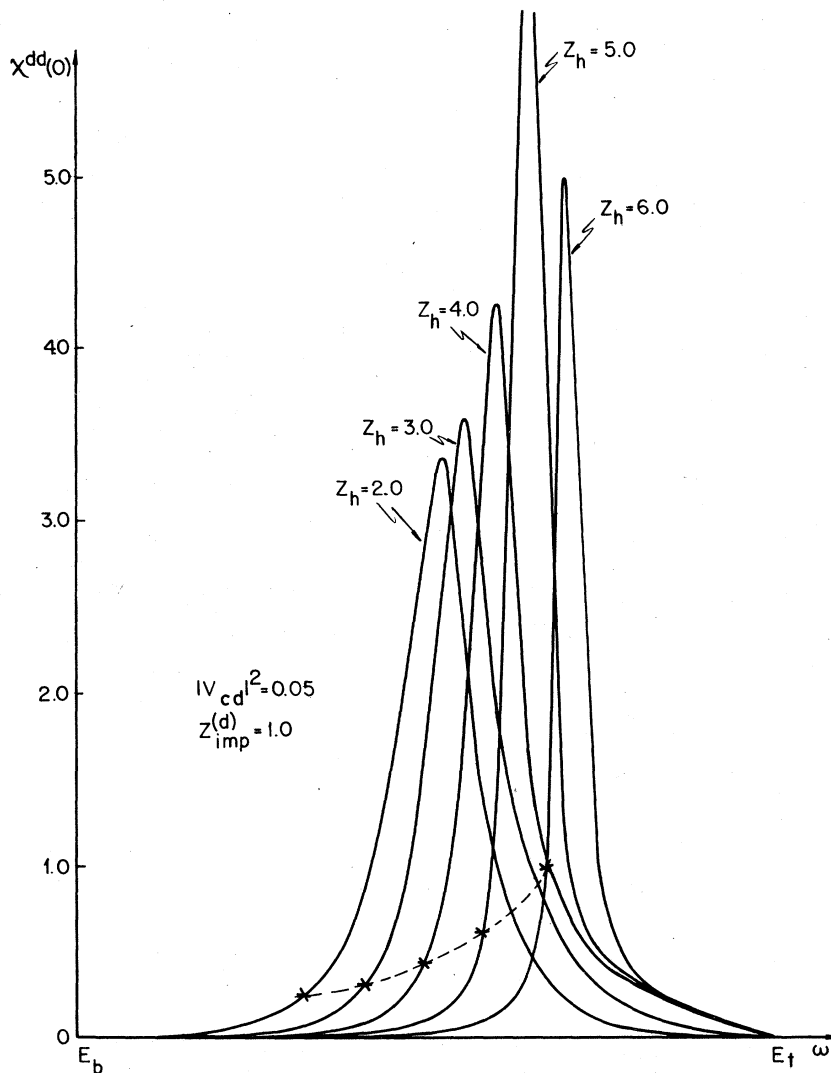


Fig. 4. (Continued)

increases along the series, thus compensating for  $J^{(d)}/J^{(c)} > 0$ , the decrease of  $\chi^{cc}(0)$ . Hence, the final result  $\chi^{cc}(0)$  [cf. (4.2)] turns out to be roughly constant and positive, as observed in Fig. 7.

Therefore, the change in sign of the total self-polarization field is to be ascribed to the competing mechanism between  $d$ -core and contact (conduction) contributions, the negative sign at the end of the series reflecting the dominance of the  $d$  over the conduction contribution. So, trivalent-rare-earth impurities in heavy  $s$ - $p$  metals show the asimilar behavior of rare-earth impurities in transition hosts<sup>6</sup> in the sense that  $d$ -core polari-

zation contribution dominates over the contact one.

We have checked numerically the importance of the choice of the ratio  $J^{(d)}/J^{(c)}$  in the final results (4.3). It turns out that, due to compensations, varying  $J^{(d)}/J^{(c)}$  from 1 to 2 does not lend to striking differences in the final results. In Fig. 8 we report the numerical results for the self-polarization field in the case where  $J^{(d)}/J^{(c)} < 0$ , the  $J^{(d)}$  coupling being a positive one. We adopt  $|J^{(d)}/J^{(c)}| = 2$  and we consider three values for  $|V_{cd}|^2$  as in the case discussed in Fig. 7. Comparison between Figs. 7 and 8 shows that the  $d$ -core polarization in both cases are not so different. This is because

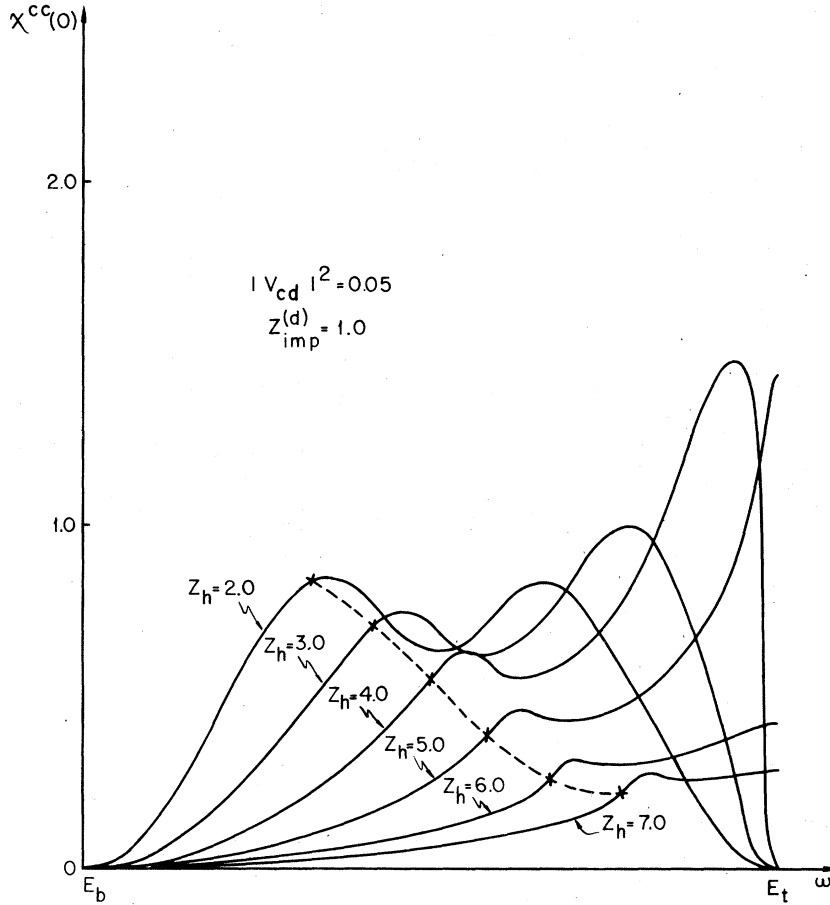


FIG. 5.  $c$ - $c$  local magnetic susceptibility  $\chi^{cc}(0)$  as a function of energy for the band model (4.1).  $|V_{cd}|^2 = 0.05$  and the SK potentials which correspond to the various values of  $Z_h$  are self-consistently obtained through (2.4). The dotted lines joining the crosses give the self-consistent values of  $\chi^{cc}(0)$  along the  $s$ - $p$  series.

a change of sign of the ratio appears only through the factor  $J^{(c)}/J^{(d)}$ , which is small for the adopted value. However, if the ratio  $|J^{(d)}/J^{(c)}|$  approaches 1, strong deviations occur, since in this case the correction factor  $1 + (J^{(c)}/J^{(d)})\chi^{\text{mix}}(0)/\chi^{dd}(0)$  may even change sign. We have checked this behavior numerically and it indeed occurs. The contact contribution as illustrated in Fig. 8 shows a monotonically increasing behavior and this is because a competitive mechanism is present. In fact, since  $J^{(d)} > 0$ , from (4.2) one sees that  $H_{\text{hf}}^{(c)}/J^{(c)}A_{\text{eff}}(Z)\langle S^z \rangle$  is a sum of an increasing part  $[-\chi^{cc}(0)]$  and an almost constant part  $[-(J^{(d)}/J^{(c)})\chi^{\text{mix}}(0)]$  which is positive and dominates at the end of the series. Thus producing the monotonic behavior.

Let us consider now the case of divalent-rare-earth impurities (such as  $\text{Eu}^{2+}$ ) in  $s$ - $p$  hosts. We claim that an  $\text{Eu}^{2+}$  impurity in  $s$ - $p$  hosts provides a physical realization of an almost pure SK contribution to the self-polarization field. In the light of the above discussion of the principles of our self-consistency procedure we have calculated the

self-polarization field for this case imposing  $Z_{\text{imp}}^{(c)} = 2$  and  $Z_{\text{imp}}^{(d)} = 0$ , i.e., no  $d$  states exist in the ionic limit of  $\text{Eu}^{2+}$ .

The total hyperfine field in this case is given by

$$\frac{H_{\text{hf}}^{(\text{tot})}}{J^{(c)}A_{\text{eff}}(Z)\langle S^z \rangle} = \bar{\chi}^{cc}(0) = \chi^{cc}(0) \quad (4.4)$$

and all  $d$  states are empty. Consequently the above-mentioned depression of  $\chi^{cc}(0)$  due to AM hybridization is irrelevant. One is involved only with the low-energy part of the  $\chi^{cc}(0)$  curve of Fig. 5, which shows the normal SK decrease of  $\chi^{cc}(0)$  for repulsive potentials driven by  $\Delta Z = Z_{\text{imp}}^{(c)} - Z_h$ . So the  $|V_{cd}|^2$  induced compensation effect which occurs for trivalent-rare-earth impurities through  $5(J^{(d)}/J^{(c)})\chi^{\text{mix}}(0)/\chi^{cc}(0)$  [cf. (4.2)] is absent and the total hyperfine field in this case decreases or increases slowly depending on whether  $J^{(c)}$  is positive or negative. This general behavior is shown in Fig. 9.

Based on the analysis of Fig. 9 we want to suggest that an experimental test of the sign of  $J^{(c)}$

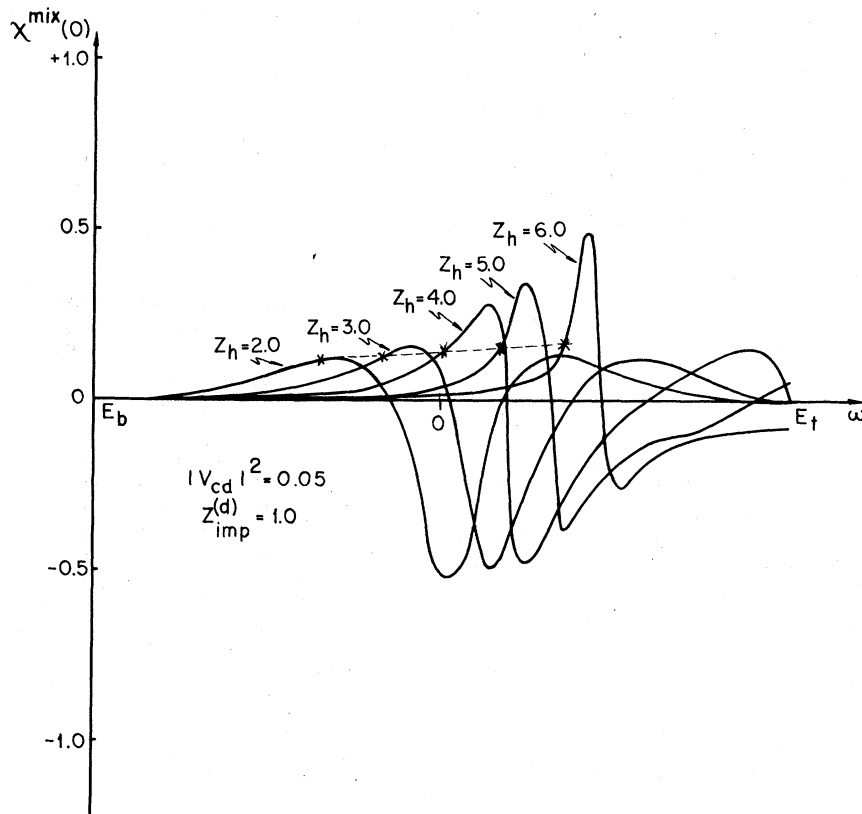


FIG. 6. Cross susceptibility  $\chi^{\text{mix}}(0)$  as a function of energy for the band model (4.1) for several self-consistent values of  $V_{cc}$  corresponding to  $Z_h$  ranging from 2 to 6.  $|V_{cd}|^2$  is taken to be 0.05 and the self-consistent values of  $\chi^{\text{mix}}(0)$  are given by the dotted lines.

along the series is provided by putting  $\text{Eu}^{2+}$  impurities in  $s$ - $p$  metals. In fact, if  $J^{(c)}$  is to change sign along the series, the slope of the hyperfine field as function of  $Z_h$  should change sign.

Another possible check of the picture for  $\text{Eu}^{2+}$  impurities in  $s$ - $p$  hosts could be provided by skew scattering measurements. In fact,  $\text{Eu}^{2+}$  is an  $S$ -state ion and according to our model the  $d$  hump is empty. So, only a small skew scattering is expected to occur, thus contrasting with  $\text{Gd}^{3+}$  impurities put in the same hosts.

## V. FINAL RESULTS

Let us summarize our principal results. First we suggest that a rare earth impurity in an  $s$ - $p$  host is a physical realization of an AM  $d$  resonance on a strongly SK perturbed  $s$ - $p$  host. This is to be contrasted to the case of the same rare earth diluted in a transition-like host<sup>5,6</sup> where  $d$ -states are already present in the host forming a  $d$ -character band. Therefore, maintaining the same rare earth probe and going from the transition series to the  $s$ - $p$  series, although one keeps a strong local perturbation, one passes from a

perturbed  $d$ -band scheme to an AM  $d$ -resonance. Both these problems are physical realizations of an impurity charge potential and a spin potential located at the same site, i.e., a limiting case of the Blandin-Campbell<sup>21</sup> problem when the separation of the charge and spin potentials tends to zero.

Peculiar effects associated to the strong SK scattering in modifying the usual AM resonant phase shift are discussed in a quite detailed form in Sec. IV A. However, those effects should be observed only for rather large fillings of the  $d$  hump. So due to the trivalent character of the magnetic rare earths (occupation of the  $d$  hump by a small number of  $d$  electrons) those unfamiliar results are expected to be absent.

A possible candidate to observe simultaneously strong conduction electron scattering (important in providing relaxation for an ESR experiment) could be provided by Mn impurities in Sb or Sn. In fact, a strong repulsive potential is expected to act in the  $s$ - $p$  host, (e.g.,  $\Delta Z_c = 3$  for Sb host) and the  $d$  hump should be occupied by  $5d$  electrons. Also, since these hosts are at the end of the  $s$ - $p$  series (i.e., a Fermi level near the top of the  $s$ - $p$  band), we expect that the unfamiliar results dis-

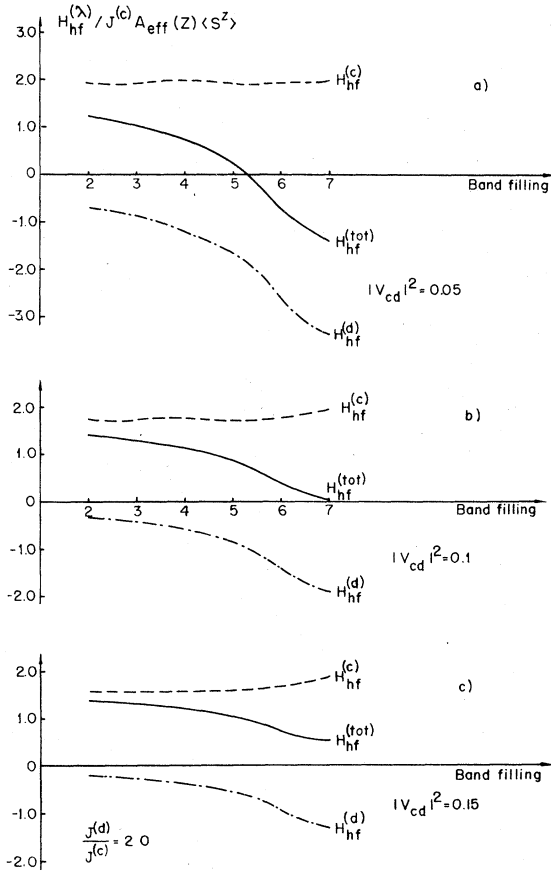


FIG. 7. Total hyperfine field, contact contribution to the field (dotted line), and  $d$ -core polarization contribution (dot-dash line) in units of  $J^{(c)}A_{\text{eff}}(Z)\langle S^z \rangle$  as a function of the band filling ( $Z_h$  ranges from 2 to 7). One takes  $J^{(d)}/J^{(c)}=2$  and  $A_{cp}^{(d)}/A_{\text{eff}}(Z)=\frac{1}{4}$ . The fields are plotted for several values of  $|V_{cd}|^2$ .

cussed in Sec. IV A are closest to be detectable.

Concerning self-polarization hyperfine results apart from the conclusions reported in Sec. IV B, we emphasize again two points, namely, (i)  $\text{Eu}^{2+}$  impurities in  $s$ - $p$  hosts could be an experimental tool to investigate the sign and magnitude of the  $J^{(c)}$  exchange coupling. Moreover, these impurities could provide an experimental test of our assumptions about the construction of the SK potential. (ii)  $\text{Gd}^{3+}$  impurities in  $s$ - $p$  hosts is suggested throughout to produce changing self-polarization hyperfine fields along an  $s$ - $p$  series. If this turns out to be true experimentally, the strength of the hybridization parameter  $|V_{cd}|^2$  could be another mechanism as compared to Blandin-Campbell<sup>21</sup> and Daniel-Friedel<sup>22</sup> source of sign changing

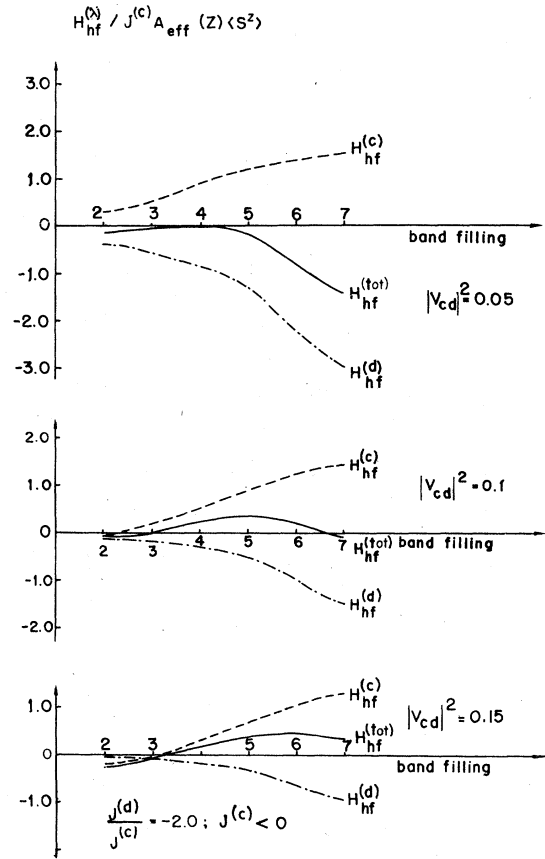


FIG. 8. Total hyperfine field, contact contribution to the field (dotted line), and  $d$ -core polarization contribution (dot-dash line) in units of  $J^{(c)}A_{\text{eff}}(Z)\langle S^z \rangle$  along the  $s$ - $p$  series for  $J^{(c)} < 0$ . One considers  $|J^{(d)}/J^{(c)}| = 2$  and  $A_{cp}^{(d)}/A_{\text{eff}}(Z)=\frac{1}{4}$ . The fields are plotted for several values of  $|V_{cd}|^2$ .

hyperfine fields, involving, however, different symmetries  $d$  and  $s$ - $p$ .

Some remarks concerning the connection of our theoretical results and possible experiments are in order. In our general expressions (4.2) and (4.3), the hyperfine field is obtained in units of  $J^{(c)}A_{\text{eff}}(Z)\langle S^z \rangle$ . To avoid the numerical estimate of the quantity  $J^{(c)}A_{\text{eff}}(Z)$  we suggest the following way for plotting the experimental results and subsequently checking the consistency of the model. Suppose one has experimental results for  $H_{\text{hf}}^{(\text{tot})}$  for a series of  $s$ - $p$  host metals, with atomic numbers  $Z_h$ . One elects a particular host of atomic number  $Z_{h_0}$  and plots  $H_{\text{hf}}^{(\text{tot})}(Z_h)/H_{\text{hf}}^{(\text{tot})}(Z_{h_0})$  as a function of  $Z_h$ . Clearly this curve should pass through the value 1 for  $Z_h = Z_{h_0}$ . The theoretical

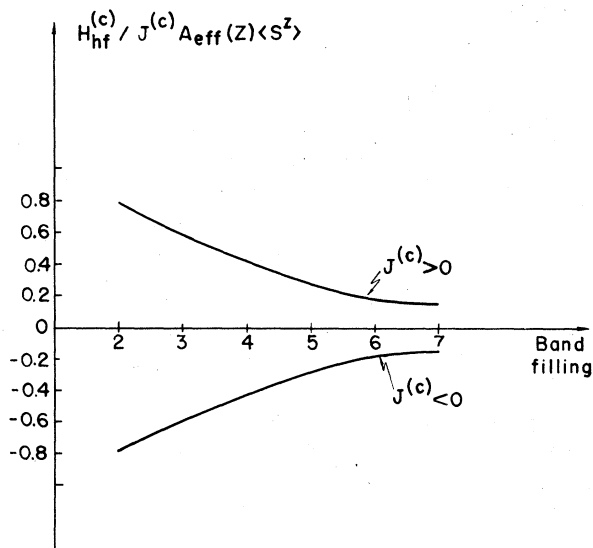


FIG. 9. Total hyperfine field in units of  $J^{(c)} A_{\text{eff}}(Z) \langle S^z \rangle$  along the  $s$ - $p$  series for the band model (4.1) perturbed by the SK potential. No  $d$  resonance is included (case of  $\text{Eu}^{2+}$ ). One considers positive and negative effective values for  $J^{(c)}$ .

results of Figs. 7–9 are then correspondingly normalized and comparison to experimental results depends now only on the parameters  $A_{\text{cp}}^{(d)}/A_{\text{eff}}(Z)$ ,  $J^{(d)}/J^{(c)}$  (as discussed in Sec. IV B) and of the strength of the  $|V_{cd}|^2$  matrix element.

Finally the above-mentioned hyperfine measurements if complemented by making Mössbauer-isomer-shift experiments and measurements involving density of states at the Fermi level such as electronic specific heat, residual, and spin-disorder resistivity would provide new tests and guides for the choice of the relevant parameters of the simple model developed in this work. Theoretical studies on the isomer-shift behavior<sup>23</sup> and Fermi-level properties<sup>24</sup> for the systems discussed in this paper are now in progress.

#### ACKNOWLEDGMENTS

It is a pleasure to thank Dr. P. M. Bisch for enlightening discussions on this subject during the stay of two of the authors (A.T. and A.A.G.) at Orsay.

- <sup>1</sup>R. Orbach, M. Peter, and D. Shaltiel, in Proceedings of the Conference on EPR of Magnetic Ions in Metals, Haute-Nendaz, 1973 (unpublished), p. 9.
- <sup>2</sup>R. H. Taylor, *Adv. Phys.* **24**, 681 (1975).
- <sup>3</sup>L. Niesen, *Hyperfine Interact.* **2**, 15 (1976); L. Niesen, P. J. Kikkert, and H. De Waard, *Hyperfine Interact.* **3**, 109 (1977).
- <sup>4</sup>K. H. Buschow, *Rep. Progr. Phys.* **40**, 1179 (1977).
- <sup>5</sup>P. M. Bisch, A. Troper, and A. A. Gomes, *Phys. Rev. B* **13**, 3902 (1976).
- <sup>6</sup>A. Troper, P. Lederer, A. A. Gomes, and P. M. Bisch, *Phys. Rev. B* (to be published).
- <sup>7</sup>See, for instance, D. Davidov, R. Orbach, C. Rettori, D. Shaltiel, and B. Ricks, *Phys. Lett. A* **35**, 339 (1971); *Solid State Commun.* **10**, 451 (1972).
- <sup>8</sup>R. Riedinger, *J. Phys. F* **1**, 39 (1971); **3**, 967 (1973); C. L. Cook and P. V. Smith, *ibid.* **4**, 1344 (1974); P. Steiner, H. Höchst, and S. Hüfner, *ibid.* **7**, L105 (1977).
- <sup>9</sup>A. Fert and A. Friederich, *Phys. Rev. B* **13**, 397 (1976).
- <sup>10</sup>J. Kondo, *Prog. Theor. Phys.* **27**, 702 (1962).
- <sup>11</sup>H. C. Chow, *J. Phys. F* **1**, 539 (1971); *Phys. Rev. B* **7**, 3404 (1973).
- <sup>12</sup>P. W. Anderson, *Phys. Rev.* **124**, 41 (1961).
- <sup>13</sup>J. C. Slater and G. F. Koster, *Phys. Rev.* **95**, 1167 (1954); G. F. Koster and J. C. Slater, *ibid.* **96**, 1208 (1954).
- <sup>14</sup>T. Moriya, *Prog. Theor. Phys.* **34**, 329 (1965).
- <sup>15</sup>C. Rettori, D. Davidov, R. Orbach, E. P. Chock, and B. Ricks, *Phys. Rev. B* **7**, 1 (1973).
- <sup>16</sup>I. A. Campbell, *J. Phys. C* **2**, 1338 (1969).
- <sup>17</sup>J. Friedel, F. Gautier, A. A. Gomes, and P. Lengart, in *Quantum Theory of Atoms, Molecules and the Solid State* (Academic, New York, 1966), p. 455.
- <sup>18</sup>J. R. Iglesias-Siccardi, A. A. Gomes, R. Jullien, B. Coqblin, and F. Ducastelle, *J. Low Temp. Phys.* **27**, 593 (1977).
- <sup>19</sup>P. W. Anderson and A. M. Clogston, *Bull. Am. Phys. Soc.* **6**, 124 (1961).
- <sup>20</sup>R. E. Watson and A. J. Freeman, *Phys. Rev.* **152**, 566 (1966); **178**, 725 (1969).
- <sup>21</sup>A. Blandin and I. A. Campbell, *Phys. Rev. Lett.* **31**, 51 (1973); I. A. Campbell and A. Blandin, *J. Magn. and Magn. Mater.* **1**, 1 (1975).
- <sup>22</sup>E. Daniel and J. Friedel, *J. Phys. Chem. Solids* **24**, 1601 (1963); E. Daniel, in *Hyperfine Interactions*, edited by A. J. Freeman and R. B. Frankel (Academic, New York, 1967), p. 712; P. Jena and D. J. W. Geldart, *Solid State Commun.* **15**, 139 (1974).
- <sup>23</sup>A. Troper, O. L. T. de Menezes, E. Fantini, D. Guenzburger, and A. A. Gomes (unpublished).
- <sup>24</sup>A. Troper, O. L. T. de Menezes, and A. A. Gomes (unpublished).